Full title:

Change-of-mind neuroeconomic decision-making is modulated by LINC00473 in medial prefrontal cortex in a sex-dependent manner

Short title:

Neuroeconomic decision-making in males and females

Authors:

Romain Durand-de Cuttoli[1], Orna Issler[2], Samantha M. B. Pedersen[4], Benjamin Yakubov[3], Nusrat Jahan[3], Aisha Abid[3], Susanna Kasparov[3], Kastalia Granizo[3], Sanjana Ahmed[3], Scott J. Russo[1], Eric J. Nestler[1,4], Brian M. Sweis*[1,4]

*Corresponding: brian.sweis@mountsinai.org

Affiliations:

[1] Nash Family Department of Neuroscience, Friedman Brain Institute, Icahn School of Medicine at Mount Sinai, New York, NY 10029

[2] Neuroscience Institute, Department of Anesthesiology, Perioperative Care and Pain Medicine, and Department of Neuroscience and Physiology, NYU Langone, New York, NY 10016

[3] CUNY Hunter, New York, NY 10023

[4] Department of Psychiatry, Friedman Brain Institute, Icahn School of Medicine at Mount Sinai, New York, NY 10029

Abstract:

Changing one's mind involves re-appraisals between past-costs versus future-value and may be altered in psychopathology. Long intergenic non-coding RNA LINC00473 in medial prefrontal cortex (mPFC) can induce stress-resilience in a sex-dependent manner, but its role in cognition is unknown. We characterized decision-making behavior in male and female mice in the neuroeconomic paradigm Restaurant Row following virus-mediated expression of LINC00473 in mPFC. Mice foraged for food among varying temporal-costs and subjective-value while on a limited time-budget. Without affecting primary deliberative decisions, LINC00473 selectively influenced re-evaluative choices in a sex-dependent manner. This included changing how mice (i) cached value with the passage of time and (ii) weighed prior mistakes, which underlie the computational bases of sensitivity to sunk costs and regret. These findings suggest a common value function is shared between these neuroeconomic processes and reveal a bridge between molecular drivers of stress-resilience and psychological mechanisms underlying sex-specific proclivities in negative rumination.

Introduction:

Understanding the mechanisms by which an individual changes one's mind when making choices is a complex psychological phenomenon that has recently gained heightened attention in the field of decision science [1]. Change-of-mind decisions involve re-evaluative, secondary processing of recently selected choices. These types of choices may be motivated by several factors, including attempts to correct recent decisions. Investigating these behaviors presents a unique opportunity to peer into how the brain represents internal conflict at multiple levels [2,3]. Conflict can be engaged at both the economic and psychological levels. The economic level may seek to manage ongoing expenditures while both minimizing potential losses and maximizing future gains [4]. The psychological level may be more focused on self-criticism of one's own recent actions, which may be useful for learning but could be perceived as unpleasant or egodystonic [5-7]. Aspects of these processes could contribute to one's affective burden and may manifest as changes in both mood and cognition observed in psychiatric disorders [8,9].

Depression is a debilitating mental illness characterized by pervasive mood disturbances, altered cognitive capabilities, and maladaptations in motivated behavior [9]. The incidence of depression is two times higher in women than in men and can manifest different symptomatology, including increased negative rumination in females [10]. However, the biological mechanisms mediating these sex differences remain unclear [11-15]. Progress has been made toward developing animal models of aspects of negative rumination. This has included breakthroughs in capturing across species the behavioral and neurophysiological signatures of regret processing [counterfactual representations of missed opportunities] and sunk costs [sensitivity to irrecoverable losses], both of which hinge on change-of-mind behavior and can drive negative rumination [5,16-18]. However, it remains unclear how psychiatric vulnerabilities in negative rumination depend on the neuroeconomic principles underlying change-of-mind decision-making. Investigating the neurobiology of sex differences in depression using this framework can not only better link changes in mood to behavior, but also provide a refined perspective on decision-making computations. This includes examining how, for instance, regret and sunk cost sensitivity relate to one another.

65 Progress is being made toward appreciating the neuroanatomical, genetic, epigenetic, and
66 pathophysiological differences between depressed males and females [19,20]. Clinical and preclinical studies
67 using sex as a biological factor have adopted innovative approaches leveraging unsupervised analyses of
68 large datasets leading to recent breakthroughs in systems biology. This has included identifying key
69 regulatory roles of non-coding elements of the genome [21]. Recent transcriptomics work carried out in human
70 postmortem brain tissue samples obtained from subjects carrying a diagnosis of major depressive disorder
71 discovered sex-dependent functions of a long intergenic non-coding RNA: LINC00473 [22]. Overall, long non-
72 coding RNAs represent a substantial percentage of all of the regulated transcripts in human depression
73 and are regulated in a sex- and brain region-specific manner [22]. Lower LINC00473 expression levels were
74 found in the medial prefrontal cortex (mPFC) of depressed females only, while there were no differences
75 observed in expression levels between healthy males and females [22]. Some studies have implicated
76 LINC00473 in molecular scaffolding, inter-organelle communication, and transcriptional regulation in non-
77 neuronal tissue, while exhibiting immediate early gene-like properties in cultured neurons. However,
78 LINC00473 function remains largely unknown with no identified role in cognition [23-28].
79
80 Studies in mice demonstrated that virus-mediated expression of LINC00473 in mPFC neurons
81 promoted resilience to stress in females only [22]. This included ameliorating depressive- and anxiety-like
82 behavioral abnormalities, while blunting hypothalamic-pituitary-adrenal-axis activity as well as the induction
83 of gene expression changes induced in this brain region by chronic stress [22]. Beyond this, LINC00473 has
84 not been studied in neural tissue in any other capacity, with no work performed to date on the role of long
85 non-coding RNAs in regulating decision-making. LINC00473 has been shown to be regulated by conserved
86 Ca^{2+}/calmodulin signaling pathways and is likely induced by cAMP response element-binding protein
87 (CREB) [22-24,26]. CREB has long been studied through traditional candidate gene approaches and shown to
88 regulate numerous other genes involved in neuronal excitability and synaptic plasticity as well as stress
89 sensitivity [29-34]. Like LINC00473, CREB function in the mPFC has been implicated in promoting resilience
90 to stress, however, unlike LINC00473, this has been shown to be true for both males and females [22,35].
91 These reports suggest either that there must be some divergence of interacting CREB-LINC00473-
92 molecular pathways between sexes or that prior studies were limited in their ability to resolve more nuanced

93 sex differences at the behavioral level. Recently, we discovered that individual differences in susceptibility
94 vs. resilience to stress were associated with alterations in higher-order neuroeconomic decision-making
95 processes, including sensitivity to regret and sunk costs. This work led to the discovery of two distinct types
96 of regret-related behaviors, one of which depends on change-of-mind decision-making[16]. Heightened
97 sensitivity to sunk costs and change-of-mind-related regret were traits previously found to be associated
98 with stress resilience. Furthermore, CREB function in the mPFC vs. nucleus accumbens could
99 bidirectionally regulate aspects of these processes [16]. Here, we build upon these findings in order to
100 characterize baseline sex differences in neuroeconomic choice behavior and the impact of LINC00473
101 function in mPFC in order to identify sex-specific vulnerabilities in decision-making.
102
103 Strides made in the field of neuroeconomics, an area focused on understanding how the brain is
104 comprised of multiple valuation algorithms, have leveraged complex approaches in decision neuroscience
105 to quantify how circuits constrain behavior [36-39]. This encompasses characterizing multifactorial aspects of
106 motivation that operationalize reward value along several dimensions, integrate choice processes with
107 environmental circumstances, and segregate stages of a decision stream into its component parts [40-43].
108 This work includes isolating properties of change-of-mind re-evaluative decisions, and points to the mPFC
109 as a critical hub for regulating reward value, self-control, and mood [4,44-48]. Insights from neuroeconomic
110 principles offer refined approaches to investigate decision-making capable of resolving behavior into
111 discretely measurable computational units in a manner that is biologically tractable and readily translatable
112 across species [40,49,50]. This approach has yielded substantial efforts developing innovative tasks adapted
113 for use in mice, rats, monkeys, and humans [5,51-54]. The use of these translational tasks have led to
114 synergistic cross-species discoveries uncovering the behavioral underpinnings of signatures of higher-
115 order cognitive processes previously thought to be unique to humans and supported by physically
116 separable circuits in the brain [16-18,55,56]. This offers an avenue for improved models of dysfunctional decision-
117 making behavior.
118
119 Here, we examined how expression of LINC00473 in the mPFC alters multiple aspects of value-
120 based decision-making behavior in male and female mice. We leveraged our longitudinal neuroeconomic

121 foraging paradigm, Restaurant Row, to characterize complex decision-making behavior in mice transfected
122 with either AAV2-hSyn-LINC00473 or AAV2-hSyn-GFP targeting mPFC neurons. This task has been used
123 previously to access behavioral and neurophysiological mechanisms of multiple decision-making systems
124 in the brain. This includes segregating within the same trial primary decisions vs. secondary re-evaluative
125 change-of-mind decisions [5,17,57-62]. On this task, rodents must budget 30 minutes to forage for their primary
126 source of food by earning pellets at spatially fixed feeding sites ("restaurants") that differ in subjective value
127 (i.e., flavors: chocolate, banana, grape, or plain). During each trial, mice are presented with auditory cues
128 whose pitch indicates the temporal delay required to earn a reward (e.g., low pitch corresponds to a short-
129 delay, low-cost offer). Each restaurant is physically divided into a separate offer zone and wait zone.
130 Rodents must make a primary decision to accept or reject an offer in the offer zone. If the offer is accepted
131 by entering the wait zone, the tone cues investment progress by descending in pitch counting down time to
132 earn a reward, during which mice can quit at any point (**Fig. 1a**, **Supplementary Fig. 1**). Behaviors in the
133 offer zone and wait zone comprise separate valuation algorithms that have been previously linked to distinct
134 circuit functions [5,16,18,43,57-59,61,63,64]. Mice were tested daily over two months across a changing economic
135 landscape during which complex foraging strategies developed. We report sex- and LINC00473-dependent
136 changes in neuroeconomic decision-making behavior specifically tied to change-of-mind decisions in the
137 wait zone, notably with alterations in sensitivity to regret and sunk costs. These data provide deeper insights
138 into the computational processes that could be driving specific aspects of re-evaluative choice. Further,
139 these data highlight a sex-dependent role of LINC00473 function in the mPFC in only certain types of
140 decision-making behaviors.
141
142 **Results:**
143
144 *Male and female mice acquire the Restaurant Row neuroeconomic task.*
145
146 We performed virus transfection surgeries on all mice and allotted 2-3 weeks for recovery before
147 beginning the longitudinal Restaurant Row paradigm (**Fig. 1a**). During the first week of Restaurant Row
148 testing, all reward offers were fixed at 1 s only (cued by a 4 kHz tone) as mice acquired the basic structure

149 of the task (**Fig. 1a-b**). Mice had to learn to run in the correct direction in order to forage for low-cost food
150 rewards. We food-restricted all mice to the same percentage (~80-85%) of baseline free-feeding body
151 weight (**Supplementary Fig. 2**). Both males and females, regardless of GFP or LINC00473 treatment,
152 grossly traveled similar total distances across the first week (**Fig. 1c**, sex*virus: F=0.971, p=0.331). All
153 groups learned to run the same number of laps in the correct direction (**Fig. 1d**, day: F=334.219, p<0.0001;
154 sex*virus: F=2.780, p=0.104) and increase their total pellets earned (**Fig. 1e**, day: F=393.991, p<0.0001;
155 sex*virus: F=3.062, p=0.089) across the first week. All mice displayed subjective flavor preferences,
156 determined by summing end-of-session total earns in each restaurant ranked from least to most preferred
157 (**Fig. 1f**, rank: F=255.250, p<0.0001). There was a modest upward shift in earns split by flavor ranking in
158 LINC00473-treated females across the first week (**Fig. 1f**, **Supplementary Fig. 3,** sex*virus: F=3.334,
159 p=0.076). Overall, these data indicate all groups were able to demonstrate the ability to acquire the basic
160 structure of the task and forage for food in a self-paced manner without overt differences in gross locomotor
161 or feeding behavior.
162
163 *LINC00473 alters sex- and value-dependent, task-driven conditioned place preference behavior.*
164
165 Before and after the first week of behavioral testing, we characterized exploratory behavior in the
166 maze arena (**Fig. 2a-b**). That is, without any active task, we allowed mice to roam the maze freely on day
167 0 and again on day 8 of the experimental timeline (**Fig. 2b**). This allowed us to probe a conditioned place
168 preference (CPP)-like response for reward sites that developed throughout the first week of self-paced task
169 performance. We measured the number of entries into and time spent near the feeder site in each
170 restaurant's wait zone on these two probe sessions (**Fig. 2c-e**). All groups explored the arena, including
171 each restaurant, to similar degrees at baseline (day 0, ANOVA, sex*virus [entries]: F=0.259, p=0.614;
172 sex*virus [time]: F=1.155, p=0.290, **Fig. 2c**). Overall, compared to the day 0 pre-test baseline, we found
173 that during the day 8 post-test all mice increased total time spent (F=75.818, p<0.0001) and – to a lesser
174 degree – entries into the reward sites (F=8.501, p<0.01, **Fig. 2c**). We then split these metrics by restaurant
175 ranked according to day 7's task earnings and found that CPP scores (post-pre delta scores) scaled with
176 flavor preferences (rank [entries]: ANOVA, F=16.307, p<0.0001; rank [time]: F=9.829, p<0.0001, **Fig. 2f-**

177 **g**). We found significantly lower CPP scores with respect to time spent but not entries into in the wait zone
178 of the most preferred flavor in LINC00473-treated females only, despite being matched to males for
179 equivalent number of rewards earned on day 7 of the task (sex*virus*rank [time]: ANOVA, F=2.844, p<0.05,
180 **Fig. 2f-g**). This sex-dependent effect was replicated in an independent cohort of mice separately
181 transfected with a lower titer of the LINC00473-expressing AAV (**Supplementary Fig. 4**). These findings
182 highlight that mPFC LINC00473 expression can have sex-specific effects on certain types of actions during
183 reward-seeking behavior (i.e., time to exit but not enter frequency) that depend on subjective value,
184 explored in further detail below throughout the rest of Restaurant Row testing [58,65,66].
185
186 *Escalating reward-scarcity unmasks sex-dependent effects of LINC00473 on foraging profiles.*
187
188 Next, we examined how foraging behaviors changed across the subsequent weeks as we
189 increased the distribution of offer costs (rage of delays encountered) without adjusting the limited time
190 budget (30 min) mice had to forage for food (**Fig. 3a**). Thus, in this "closed-economy" system, animals must
191 adapt to the changing economic landscape of the environment as reward scarcity increased – a model of
192 economic stress we recently characterized [43]. We increased costs in a stepwise manner across blocks of
193 days (i.e., offer delays ranged from 1-5 s on days 8-12, 1-15 s on days 13-17, and finally 1-30 s on days
194 18-45, as previously published [5,43,63]). We randomly sampled costs from a uniform distribution.
195
196 As expected, we found a decrease in pellets earned in response to each stepwise change in offer
197 costs (sign test [-] on earns: day after minus day before transition, collapsed across epochs: t=-12.655,
198 p<0.0001, **Fig. 3b**). These deficits in earnings scaled with flavor preferences and were matched between
199 all groups (rank: F=6.938, p<0.001, timepoint*rank: F=3.651, p<0.01; sex*virus: F=0.016, p=0.899, **Fig. 3c-**
200 **d**, **Supplementary Fig. 5**). Across the final epoch of testing (the 1-30 s offer range period: days 18-45),
201 mice displayed a complex behavioral response profile that depended on running more laps in order to
202 increase and recover total food earnings (laps [days 18-45]: F=355.340, p<0.0001; earns [days 18-14]:
203 F=252.218, p<0.0001, **Fig. 3b-d**). All groups were matched in how much food was recovered across the
204 final epoch of testing (sex*virus: F=0.234, p=0.631, **Fig. 3d**, **Supplementary Fig. 5**). However, we found

205 that overall females displayed a greater increase in the number of laps run compared to males throughout
206 this process (sex*day: F=7.848, p<0.01, **Fig. 3b**,**f**, **Supplementary Fig. 5**).
207
208 The most striking change in choice behavior across the experiment associated with the changes in
209 laps run and rewards earned was the proportion of session time re-allocated to quitting behavior in the wait
210 zone. This metric significantly increased after each stepwise change in offer costs (timepoint*choice:
211 F=226.523, p<0.0001, **Fig. 3e**) and more prominently in females (timepoint*sex [quits]: F=11.821,
212 p<0.0001, **Supplementary Fig. 6**). Interestingly, while sex differences in wait zone quitting behavior
213 disappeared in the final epoch of testing for the GFP control group, LINC00473-treated mice instead
214 displayed a widening of sex differences in quitting behavior (sex*virus: F=8.201, p<0.01, **Fig. 3g**,
215 **Supplementary Fig. 6**). Furthermore, LINC00473-treated females displayed shorter latencies to quit in the
216 wait zone compared to males, particularly for more preferred flavors (sex*virus*day*rank: F=2.805, p<0.05),
217 despite no changes in offer zone enter frequency or offer zone reaction times (F=1.713, p=0.162,
218 **Supplementary Fig. 6**). This effect of LINC00473 in the wait zone is reminiscent of the changes in female
219 behavior during the CPP probe sessions (see **Fig. 2**). Taken together, these data reflect rearrangements
220 in complex foraging patterns that emerged across longitudinal time scales in response to worsening
221 economic demand. Changes in laps run and rewards earned were ultimately driven by more rigorous
222 quitting behavior in LINC00473-treated females. These analyses reveal sex-dependent effects of mPFC
223 LINC00473 expression that alter quit frequency and quit reaction times, which were not unmasked until
224 mice encounter a reward-scarce environment.
225
226 *Change-of-mind decision-making patterns reveal unique sex-dependent neuroeconomic policies.*
227
228 To characterize the economic nature of the decisions made in the offer zone and wait zone, we
229 quantified decisions to enter vs. skip (offer zone) or earn vs. quit (wait zone) as a function of both the cued
230 offer cost and flavor identity (**Fig. 4a-c**). All groups were capable of making cost-informed enter vs. skip
231 choices in the offer zone or earn vs. quit choices in the wait zone. Meaning, all mice were able to
232 discriminate tones when making choices (offer*flavor [offer zone]: F=13.129, p<0.001; offer*flavor [wait

zone]: F=18.006, p<0.001, **Fig. 4c**). Furthermore, how offer costs altered enter vs. skip and earn vs. quit probabilities scaled with flavor preferences in all groups (**Fig. 4b**). To summarize these behaviors, we calculated thresholds of willingness to enter in the offer zone and, separately, willingness to wait to earn a reward in the wait zone by fitting a Heaviside step regression to the trial outcome as a function of the delay that is cued at the start of each trial (note: this metric does not include reaction time or latency to make the choice). We then extracted the inflection point in each restaurant (**Fig. 4d, inset**). Thus, these measures capture the offer cost at which 50% of trials are entered in the offer zone and, separately, earned in the wait zone.

Overall, in all groups, we found that offer zone thresholds significantly differed from wait zone thresholds across epochs of testing (timepoint*zone: F=296.648, p<0.0001, **Fig. 4d**). Upon transitioning to the 1-30 s epoch (day 18), offer zone thresholds drastically increased in all groups to similar degrees while retaining the ordinal ranking of flavor preferences (rank: F=17.247, p<0.0001; sex: F=0.170, p=0.681; sex*virus: F=0.031, p=0.861, **Fig. 4d-f**). Wait zone thresholds, on the other hand, increased only in male mice following the transition to the 1-30 s epoch (rank: F=58.574, p<0.0001; sex: F=17.776, p<0.0001; sex*virus: F=1.238, p=0.268, **Fig. 4d-f**). Over the subsequent week (approximately days 18-24), wait zone thresholds in males decreased before stabilizing across the remainder of the experiment (approximately days 25-45, **Fig. 4d-f**). In females, wait zone thresholds (i) remained relatively unchanged upon transition to day 18, (ii) were significantly lower than males, and (iii) remained stable across the entire 1-30 s epoch (sex*rank [offer zone]: F=0.484, p=0.694; sex*rank [wait zone]: F=3.689, p<0.05, **Fig. 4d-f**). Offer zone thresholds on the other hand remained equal in all groups and gradually decreased across a much slower timescale over several weeks (**Fig. 4d-f**). LINC00473 expression in mPFC did not significantly alter any decision-making thresholds (sex*virus [offer zone]: F=1.781, p=0.185; sex*virus [wait zone]: F=187, p=0.175, **Fig. 4d-f**).

In order to determine which groups' decision policies were most optimal, we leveraged an economic analysis we recently developed that quantifies how mice maximize food and subjective value [43]. This analysis takes each animal's offer zone and wait zone thresholds observed on each day and calculates the

261 Euclidean distance between these observed thresholds and theoretical thresholds that yield either the most
262 amount of food or most amount of subjective value (see **Methods** and **Supplementary Fig. 7**). In the 1-30
263 s epoch, we empirically determined through computer simulations that a threshold of 10 s in any restaurant
264 yields the most amount of food [43]. Observed thresholds that are either above or below this theoretical
265 threshold thus are suboptimal, in the food-maximizing domain. To determine theoretical thresholds that
266 maximize subjective value, we used individual differences in flavor-specific earnings on day 7 when all
267 costs were 1 s only [43]. This allowed us to determine idealized thresholds in each restaurant in the 1-30 s
268 epoch that re-approximates on a mouse-by-mouse basis day 7's ratio of earnings across flavors [43].
269 Therefore, observed thresholds that are either above or below this theoretical threshold thus are
270 suboptimal, in the subjective value-maximizing domain. Euclidean distances between observed and
271 theoretical thresholds were calculated separately in the offer zone and wait zone using a 4-dimensional
272 vector of thresholds comprising each restaurant [chocolate, banana, grape, plain].
273
274 We found that female decision-making policies in the final epoch of testing were more optimized
275 for both maximizing total food intake as well as maximizing subjective value compared to males (**Fig. 4g-i**,
276 **Supplementary Fig. 7**). This sex-dependent effect was specific to wait zone but not offer zone decision-
277 making policies. LINC00473 treatment had no effect on Euclidean distances. These data highlight a robust
278 sex difference in the optimality of wait zone decision-making policies unique from those in the offer zone
279 [16,57]. The fact that thresholds are not altered by LINC00473 rules out major confounds of baseline
280 willingness to enter or willingness to wait on higher-order change-of-mind decision-making valuations
281 investigated further below.
282
283 *LINC00473 alters the temporal dynamics of change-of-mind decision-making behavior.*
284
285 Wait zone thresholds capture economic indifference points of re-evaluation decisions when
286 deciding to stay or quit. We defined these measures by choice outcome as a function of the offer cost that
287 was cued at trial start, that is, at the onset of the countdown during the delay period. Next, we quantified
288 more dynamically at what timepoint quit decisions were made during the delay period in the wait zone. We

289 calculated the value of each offer as well as the value remaining in the countdown at the moment of quitting.
290 We subtracted the offer or countdown time remaining from an individual mouse's wait zone threshold in
291 each restaurant (example trial: 18 s offer entered, mouse's threshold = 10 s, **offer value** = 10 - 18 **= -8**,
292 latency to quit = 4 s, time remaining at quit = 14 s, **value remaining** at quit = 10 - 14 = **-4**, **Fig. 5a,**
293 **Supplementary Fig. 8**). We found all mice generally made quit decisions for accepted offers that were (i)
294 typically above one's wait zone threshold (i.e., negatively valued offers) and (ii) had ample time remaining
295 in the countdown such that the remaining time investment required to obtain the reward was still above
296 one's threshold (i.e., negative value left, **Fig. 5a**). Therefore, most quit decisions are economically
297 advantageous and are efficiently time-saving (**Fig. 5a**). Furthermore, quit decisions are corrective re-
298 evaluations of sub-optimal and impulsive offer zone decisions, consistent with previous reports [5,16,43,56,58].
299 Importantly, groups did not differ in how they made enter vs. skip decisions in the offer zone
300 (**Supplementary Fig. 9**).
301
302 We found that females made quit decisions in the wait zone with significantly lower and more
303 negative value remaining in the countdown compared to males (sex*virus: F=195.823, p<0.0001, **Fig. 5b**).
304 This sex difference was more pronounced in LINC00473-treated animals (sex*virus: F=12.957, p<0.001,
305 **Fig. 5b**). Furthermore, only LINC0047-treated mice revealed a sex difference in the number of quit
306 decisions that could be characterized as economically advantageous (as described above, sex*virus:
307 F=153.236, p<0.0001). There was a greater proportion of these events in females relative to males and
308 compared to other quit events that were less common and more disadvantageous (i.e., (i) quitting negatively
309 valued offers [above one's threshold] with positive value left [below one's threshold]; or, (ii) quitting
310 positively valued offers [below one's threshold]; both (i) and (ii) reflect quits passing a timepoint after which
311 mice should have chosen to stay instead, quit type*sex*virus: F=13.293, p<0.0001, **Fig. 5c-d,**
312 **Supplementary Fig. 8**). Overall, these data indicate that LINC00473-treated females engage in more
313 economically advantageous change-of-mind decisions compared to males that depend on the temporal
314 dynamics and efficiency of quitting behavior.
315

316 Next, we characterized sensitivity to sunk costs while mice made continuous re-evaluation
317 decisions in the wait zone as a function of the passage of time (which wait zone thresholds do not capture).
318 We calculated the instantaneous probability of staying and earning a reward in the wait zone as a
319 continuous function of not only (i) the time remaining in the countdown at each snapshot in time but also
320 (ii) the time already spent waiting [18]. We computed a survival analysis using a sliding 1 s window after
321 binning all trials of varying starting offers into [*time spent*, *time left*] pairs (**Fig. 5f**). We then calculated the
322 probability of earning a reward as a function of time already spent waiting independent of temporal distance
323 to the goal (see **Methods** and **Supplementary Fig. 8** for a detailed and graphical description of sunk cost
324 analyses and control analyses).
325
326 In all groups, we found that the passage of time drove an increased likelihood that mice would
327 continue to wait – an escalation of commitment – which grew additively stronger with more time spent (time
328 spent*time left: F=891.924, p<0.0001, **Fig. 5f-h**). This effect was independent of and orthogonal to temporal
329 distance to the goal measured at any given moment in time. We found a significant sex difference in
330 sensitivity to the amount of time already spent waiting only in LINC00473-treated mice. LINC00473-treated
331 females demonstrated increased sensitivity to sunk costs, while LINC00473-treated males instead
332 demonstrated relatively diminished sensitivity (sex*virus: F=15.944, p<0.0001, **Fig. 5i**). Sunk cost
333 sensitivity only emerged after mice transitioned to the 1-30 s epoch (time spent in wait zone [1-15 s offers]:
334 F=0.174, p=0.677, **Fig. 5i**, **Supplementary Fig. 10**). Sunk cost sensitivity uniquely affected wait zone
335 decisions compared to other forms of time spent on this task, including in the offer zone (time spent in offer
336 zone: F=0.558, p=0.455; time spent*sex*virus: F-0.418, p-0.518, **Supplementary Fig. 10**, see
337 **Supplementary Text** and **Supplementary Fig. 11-13** for manipulations of task-relevant sensory
338 information).
339
340 These data describe how LINC00473-treated females are more sensitive to the passage of time
341 when re-evaluating the decision to quit. This captures a critical duplexity: although LINC00473-treated
342 females are generally more likely to engage in rapid, economically advantageous quit decisions, they also
343 change in this regard more dynamically with the passage of time. That is, LINC00473-treated females cache

344 more value with time spent when deciding to quit that promotes overstaying behavior. This reflects a
345 steepened value function during the re-evaluation process that is capable of overturning quit choices during
346 change-of-mind decision-making, enhanced by mPFC LINC00473 expression in females.
347
348 *LINC00473 alters the impact of prior change-of-mind decisions on future behavior.*
349
350 Next, we aimed to characterize how sequences of events surrounding quit decisions influenced
351 subsequent behavior. Because trials are interdependent, a strength of the Restaurant Row foraging task
352 lies in being able to subdivide trial sequences into unique economic scenarios in which animals
353 naturalistically find themselves. We identified trial pair sequences [trial t-1 → trial t] in which animals made
354 atypical, economically suboptimal choices [on trial t-1] and measured the change in economic choice
355 behavior on the next trial [on trial t: the read-out trial] [5,16,17]. These events were compared to specific
356 alternative sequences that control several additional variables on both trial t-1 and trial t in order to rule out
357 other confounds and isolate the economic impact of choice history on future behavior: (i) the value of the
358 offer presented, (ii) the flavor identity, and (iii) the previous action selected. Sequences were extracted post
359 hoc from natural encounters while foraging amid randomly presented offers and not constructed a priori nor
360 built into the task design. This allowed us to investigate how past economic violations alter future choices
361 as a behavioral readout of sensitivity to regret, as previously demonstrated [5,16,17].
362
363 We previously defined two distinct sequences of events on this task that each capture the impact
364 of decision history on future choices but differ in the specific actions that give rise to two types of economic
365 violations [5,16,17]. **Scenario type 1**: situations in which animals inappropriately forgo a high-value offer [on
366 trial t-1] only to subsequently encounter a worse low-value offer on the next trial [trial t] (**Fig. 5j**). This can
367 be classified as a violation sequence and can be compared to the non-violation control sequence in which
368 mice instead appropriately accepted the high-value offer on trial t-1, holding all other variables constant
369 (**Fig. 5j**). Here, we found that all groups were behaviorally insensitive to scenario type 1, with no effect of
370 sex or LINC00473 expression (+ sign test: [male GFP]: t=-0.282, p=0.608; [female GFP]: t=0.101, p=0.461;
371 [male LINC]: t=0.521, p=0.308; [female LINC]: t=-0.144, p=0.556, **Fig. 5j**). That is, there were no changes

372 in economic choice behavior on the read-out trial when comparing violation sequences to non-violation
373 sequences [thus yielding a delta score of zero for choice probabilities on trial t] (**Fig. 5j**).
374
375 **Scenario type 2**: situations in which animals inappropriately accepted a low-value offer [on trial t-
376 1] (**Fig. 5k**). Note that these scenarios typically result in a change-of-mind decision once in the wait zone.
377 This violation sequence can be compared to the non-violation control sequence in which mice instead
378 appropriately skipped the low-value offer on trial t-1, holding all other variables constant and matched for
379 the same low-value offer on trial t as in scenario type 1 (**Fig. 5j-k**). Overall, we found that mice demonstrated
380 behavioral sensitivity to scenario type 2, whereby individuals were more likely to compensate for and accept
381 low-value offers that they typically would not accept on the read-out trial following violation sequences
382 compared to non-violation sequences (**Fig. 5k**). Interestingly, only GFP-treated females did not display
383 behavioral sensitivity to scenario type 2, while all other groups including LINC00473-treated females
384 displayed delta scores significantly greater than zero (+ sign test: [male GFP]: t=2.931, p<0.01; [female
385 GFP]: t=1.123, p=0.145; [male LINC]: t=3.056, p<0.01; [female LINC]: t=2.196, p<0.05, **Fig. 5k**).
386
387 These data reveal how mice can differentially carry the weight of distinct types of past mistakes
388 into future choices. Remarkably, there is a unique enhancement of behavioral sensitivity to type 2 but not
389 type 1 scenarios caused by mPFC LINC00473 treatment in females only. These events depend on change-
390 of-mind decisions on trial t-1 and derive from the same trial pool from which sensitivity to sunk costs is
391 measured, and importantly, enhanced in LINC00473-treated females. Taken together, this suggests a
392 common underlying computational process may be shared between change-of-mind-related regret and
393 sunk cost sensitivity that is engaged by mPFC LINC00473 expression in females, resulting in a steepened
394 value function shared across both processes. Furthermore, these findings provide an example whereby
395 LINC00473 expression in this brain region overcomes a baseline sex difference that is potentially
396 disadvantageous for females. This is especially important considering (i) LINC00473 expression in mPFC
397 carries pro-resilient properties in females and (ii) traits associated with enhanced sensitivity to type 2 regret
398 and sunk costs have been previously linked to stress-resilient individuals [16,22,43].
399

In summary, this collection of findings demonstrates the complexity of change-of-mind decisions that respond to the economic landscape of the environment. This work showcases the multifactorial ways in which re-evaluative choice processes can be uniquely modulated in a sex-dependent manner. Importantly, we highlight a distinction between separate phases along a continuous decision stream captured within the same trial: primary offer zone judgements followed by secondary wait zone re-evaluative decisions. We reveal striking sex differences and sex-dependent effects of LINC00473 expression in mPFC on only wait zone decisions. We provide evidence for LINC00473-induced changes in signatures of two different yet related higher-order decision-making phenomena during quit decisions: sensitivity to the passage of time in the form of sunk costs and change-of-mind related regret – valuation algorithms that comprise critical aspects counterfactual thinking.

410 **Discussion:**

411

412 In this study, we characterized complex behaviors in mice tested on the neuroeconomic foraging
413 paradigm, Restaurant Row. We explored the role of a non-coding RNA, a relatively poorly understood class
414 of molecules, on motivated behavior. We discovered sex-dependent effects of LINC00473 expression in
415 mPFC neurons on specific aspects of value-based decision-making behavior. This was typified by
416 selectively altering the way in which an individual changes one's mind during an ongoing re-evaluative
417 decision without affecting primary evaluations. Importantly, we discovered a role for mPFC LINC00473
418 expression – which we recently found increases stress resilience in simple behavioral screening tests in
419 female mice only [22] – in enhancing the contrast of re-evaluation processes in females. Our findings extend
420 from simple conditioned place preference behaviors like those commonly assayed using simpler goal-
421 oriented paradigms [50,67,68] to more complex, higher-order neuroeconomic phenomena. These findings build
422 upon our recent work characterizing how complex decision-making processes go awry in depression and
423 interact with molecular regulators of stress resilience [16]. Here, we provide a deeper understanding of how
424 multiple stages of a continuous decision stream derive from dissociable psychological mechanisms. We
425 explored how perturbations in change-of-mind decision-making could underlie select elements of negative
426 rumination. Our findings have important implications for how molecular determinants of stress-sensitive
427 decision-making processes interact with non-coding regions of the genome differently in the male and
428 female brain.

429

430 The distinction between offer zone choices and wait zone choices on the Restaurant Row task is
431 critically important. They reflect a separation of fundamentally distinct decision-making processes that occur
432 within the same trial but are segregated across space and time [58]. Numerous reports have tested subjects
433 on this paradigm translated for use across species in task variants adapted for mice, rats, monkeys, and
434 humans [18,51,52]. These studies have shed light on the biological and psychological implications of resolving
435 dissociable, evolutionarily conserved decision-making processes. In the offer zone, individuals engage
436 deliberative systems that represent alternating options of competing actions between which one must
437 choose [61,62]. This has been shown in rodents to derive in part from hippocampal (HPC)-dependent

438 processes [57,58]. Population-level activity of neurons in HPC can encode multiple, alternating future paths
439 through the offer zone to potential goals in the current vs. next restaurant [65,67,69,70]. Similar findings have
440 been observed from fMRI studies in humans tested on a translated version of the Restaurant Row task [55].
441 Default mode network activation patterns can encode competing future options during offer zone
442 deliberation, but seldom do such representations include past events or previous restaurants [2,71].
443
444 Decisions in the wait zone on the other hand are much less understood. The HPC has been
445 implicated in wait zone decisions as well: it switches oscillatory activity from a predominately theta-driven
446 state sensitive to the cued offer costs in the offer zone [61] instead to an increase in sharp wave ripple activity
447 sensitive to time spent waiting in the wait zone [62]. Further, wait zone decision periods also depend on HPC
448 synchrony with the mPFC [61,62]. Recordings in rodents from the mPFC on Restaurant Row surprisingly found
449 no evidence of encoding of the cued offer costs when animals were in the offer zone [59]. However, once in
450 the wait zone, mPFC neurons strongly represented offer value independent of time spent waiting and could
451 predict whether or not the trial would terminate in a quit [59]. Within the mPFC, pairs of neurons also drastically
452 changed excitation-inhibition balance specifically when animals were in the wait zone [72]. Taken together,
453 these findings indicate a qualitative shift in mental state upon transition from the offer zone to the wait zone
454 that recruits the mPFC preferentially during change-of-mind decisions.
455
456 This study represents the first analysis of females in the Restaurant Row task. Nearly all of the sex
457 differences captured here, including those altered by mPFC LINC00473 expression, are restricted to wait
458 zone and not offer zone behaviors (**Fig. 6, Supplementary Fig. 14**). Importantly, we found no effects of
459 sex or LINC00473 on how impulsive or deliberative animals behaved in the offer zone. This includes no
460 changes in vicarious trial and error behavior, which is known to correlate with neural representations of
461 episodic future thinking and model-based planning in HPC among other structures [73]. Recently, we showed
462 that LINC00473 expression diminishes spontaneous excitatory post-synaptic current frequency and
463 amplitude in excitatory mPFC pyramidal neurons of female mice, with no effect seen in males [22].
464 Chemogenetic inactivation of the mPFC during Restaurant Row diminishes wait zone quit decisions [60-62].
465 Optogenetic induction of long-term depotentiation in excitatory mPFC neurons that project to the nucleus

466 accumbens (NAc) [57], where negative dopamine reward prediction error signals have been found to causally
467 precede quit choices on Restaurant Row [64], selectively decreases quitting behavior for several days without
468 altering offer zone behavior [57]. Outside of Restaurant Row, intracranial optogenetic excitatory self-
469 stimulation of mPFC terminals in the NAc can be reinforcing while also promoting enter-then-quitting
470 behavior [74]. These converging findings suggest that LINC00473 expression is likely mediating sex-
471 dependent effects on change-of-mind decisions by at least in part dampening and restructuring mPFC
472 activity and connectivity with other regions. In depressed patients, neuromodulation interventions that
473 decrease mPFC activity yield therapeutic benefits in mood [75]. Thus, understanding how these decision-
474 making changes come together can help bridge interpretations between the behavioral and neural
475 computations underlying phenomena like negative rumination and the molecular drivers of stress
476 responses traits.
477
478 A key insight from the present study is a conceptual advance toward developing neuroeconomic
479 principles unifying two critical features of change-of-mind decision-making: sensitivity to sunk costs and
480 regret. Sensitivity to sunk costs captures a well-studied cognitive bias whereby irrecoverable past
481 expenditures can enhance the value of continuing to invest in and perseverate on an ongoing endeavor
482 instead of cutting losses, as we have reported previously captured across species [18,56]. Sensitivity to regret
483 describes how representations of missed opportunities and alternative actions that could have led to better
484 outcomes can influence future choices [5,6,16,17]. We theorize that these two phenomena share, at least in
485 some respects, a common computational origin (**Fig. 7**). We previously characterized – behaviorally and
486 neurophysiologically – distinct forms of regret based on two types of economic scenarios in which
487 individuals find themselves [5,16,17]. Type 1 scenarios describe economically risky decisions to skip high-value
488 offers, followed by poor outcomes. Type 2 scenarios describe economically poor decisions to enter and
489 begin investing time in low-value offers before deciding to quit. Counterfactual thinking during type 2
490 scenarios likely evokes “should have skipped instead” representations that drive change-of-mind decisions.
491 We posit that sensitivity to sunk costs, which derive from these same type 2 scenarios, is a parallel valuation
492 that stems from the same counterfactual process as type 2 regret and may compete with the decision to
493 quit. With the passage of time, this can promote overstaying behavior and drive sensitivity to sunk costs.

494 However, if an individual does quit, this can also drive altered valuations on the subsequent trial and
495 promote compensatory behavior, measured as type 2 regret sensitivity. Here, we provide evidence that
496 both of these processes – sensitivity to sunk costs and type 2 regret – can be experimentally enhanced in
497 LINC00473-treated females without affecting type 1 regret sensitivity or other lower-order decision
498 processes such as willingness to wait. This suggests that a value function of a common counterfactual
499 process is being selectively enhanced in these animals (**Fig. 7**). Within this conceptual framework, we posit
500 that features of negative rumination could stem from a shared neural substrate governed by these two
501 neuroeconomic processes and may be associated with stress-related traits of the individual.
502
503 To put this in context, we recently characterized the impact of chronic social defeat stress on
504 Restaurant Row behavior in male mice, in tandem with disruptions of CREB function in mPFC [16,43,76]. First,
505 we found that mice were required to progress through worsening economic challenges in order to extract
506 any group differences in foraging profiles [43]. This is consistent with results presented here that emphasize
507 the importance of considering the environmental demand and stressors of a task necessary to unmask
508 disease-relevant phenotypes. Second, we found that stress-resilient mice – defined by a simple social
509 interaction screening test measured outside of the Restaurant Row task – mounted the most robust
510 behavioral response to the transition into the 1-30 s reward-scarce environment in order to recover food
511 earnings, similar to LINC00473-treated female mice as shown here [43]. Third, without grossly altering
512 decision-making thresholds, we found striking stress-induced changes in sensitivity to sunk costs and
513 regret. Stress-susceptible mice demonstrated increased regret sensitivity to type 1 scenarios. This was a
514 phenotype no group demonstrated in the present study [16]. Additionally, stress-susceptible mice
515 demonstrated diminished regret sensitivity to type 2 scenarios. Furthermore, stress-resilient individuals
516 instead displayed enhanced sensitivity to type 2 scenarios as well as enhanced sensitivity to sunk costs [16].
517 Taken together, this suggests that the females in the present study at baseline may have a decision-making
518 vulnerability specifically in change-of-mind choice processes that is enhanced or restored to male levels by
519 LINC00473 expression in mPFC.
520

521 In our prior study, knocking down CREB function had multifactorial effects on decision-making
522 behavior depending on the brain region targeted (mPFC vs. NAc) and whether or not animals were stress-
523 naïve at baseline vs. exposed to subsequent stress [16]. CREB function in the mPFC was required to maintain
524 suppression of regret sensitivity to type 1 scenarios and, when knocked down, rendered only type 2
525 scenarios sensitive to subsequent stress. This pattern was distinct from CREB function in the NAc where it
526 is known to drive stress susceptibility [16,29,77,78]. Importantly, CREB function in mPFC altered not only re-
527 evaluative decisions in the wait zone but also primary decisions in the offer zone, including affecting
528 impulsive choices as well as deliberative vicarious trial and error behavior [16], unlike the effects of
529 LINC00473 here which were restricted to wait zone decisions only and did not alter type 1 regret sensitivity.
530
531 These data implicate a divergence in how CREB and LINC00473 interact within the mPFC to drive
532 distinct aspects of decision-making behavior. This allows for a new perspective to interpret prior findings in
533 stress research but also opens new questions for future lines of investigation. For instance, it is possible
534 that CREB and LINC00473 effects on neuronal function may diverge in different cell types or sub-
535 populations of neurons that receive different inputs or project to different downstream regions. Prior work
536 implicates involvement of HPC and NAc as two key regions that could be mediating this difference. Sex-
537 dependent effects of LINC00473 also suggest that complex interactions between sexually dimorphic circuits
538 and sex hormones may be critically important in determining how mPFC neurons encodes time, value, and
539 choice. Quantifying similarities in neural signals during the processing of sunk costs vs. distinct regret types
540 remains an open question, with explicit predictions we make here about similarities between sunk costs
541 and type 2 regret. Finally, it is unknown if the representations during the processing of sunk costs or change-
542 of-mind regret overlap with the sort of content patients with depression ruminate over and what features of
543 counterfactual thinking, if any, promote stress-resilience in humans.
544
545 Limitations of the current student include that LINC00473's sex-dependent effects on behavior
546 have only been causally tested in the mPFC to date [22]. Further, prior CREB knockdown studies during
547 Restaurant Row were conducted in males [16,43,76]. Although postmortem human tissue studies implicate
548 mPFC as a top region to investigate [22], understanding LINC00473's role in other regions, especially in how

549 it may be interacting with other key molecular players such as CREB in the NAc [26,29,30], will be critically
550 important in future studies investigating multiple networks. For instance, LINC00473 has been shown to
551 increase cellular excitability in cultured HPC neurons [26], contrary to its effects in mPFC [22]. It will be critical
552 to record *in vivo* neural activity from these structures in both males and females with and without
553 perturbations of LINC00473 alone, CREB alone, and both, in order to characterize the interplay between
554 these overlapping molecular pathways. Future decision-making studies should combine experiments of
555 LINC00473 manipulations with exposure to other stressors, beyond the economic challenges tested in the
556 present study, such as chronic social defeat or variable stress on decision-making [22]. Additional work needs
557 to be done investigating the role of gonadal steroid hormones, sex chromosomes, and sex-dependent
558 noncoding RNAs in mediating aspects of these reported sex differences. As just one example, CREB
559 function has been shown to fluctuate with estrus cycle [79-83]. Additionally, given previous reports that
560 LINC00473 expression in mPFC of stress-naïve male mice can induce behavioral changes in simpler
561 assays (i.e., marble burying) [22], it would be fruitful to explore in future work how Restaurant Row decision-
562 making profiles could relate to traits outside of the task itself (e.g., anxiety-related behavior measured on
563 independent tests).
564
565 We discovered robust sex differences in neuroeconomic change-of-mind decision-making. We
566 found that LINC00473 expression in the mPFC of females gave rise to enhanced behavioral sensitivity to
567 sunk costs and change-of-mind related regret. These effects on secondary re-evaluative choices were
568 independent of primary decisions. Counterfactual thinking during change-of-mind decisions can elicit
569 “should not have done that” mental representations that map hypothetical outcomes onto alternative actions
570 that could have been selected instead. We propose that the processing of sunk costs and change-of-mind
571 related regret may depend on a common value function and shared form of counterfactual thinking. Such
572 processes could guide aspects of negative rumination and impact mood as well as stress-resilience.
573 However, even if change-of-mind decisions are unpleasant or evoke some degree of cognitive dissonance,
574 enhancing the salience of this process could increase attention paid toward realized losses and carry utility
575 for fictive learning. Collectively, variations in these decision-making patterns are sex-dependent and may
576 alter the lens through which individuals process their past mistakes.

577 **Methods**

578 *Subjects:* Adult male and female C57BL/6J mice (Jackson, 10wks, n=40) were used. Mice were
579 individually housed and maintained on a 12-hr light/dark cycle with ad libitum water, only food-restricted
580 during Restaurant Row testing, conducted during their light phase. Experiments were approved by the
581 Mount Sinai Institutional Animal Care and Use Committee (IACUC; protocol number LA12-00051) and
582 adhered to the National Institutes of Health (NIH) guidelines.

583

584 *Viral constructs:* To achieve long-term neuronal expression of LINC00473, it was subcloned into
585 an AAV plasmid with human synapsin promoter (hSyn) driving gene expression. LINC00473 transcript
586 variant 1, (NR_026860.1 /AK289375) of 1821bp length was subcloned from p1005+ HSV vector [22] into
587 pAAV-hSyn-eGFP-hSny plasmid [83] using blunt ligation into a PMEI and EcoRV restriction sites following
588 the second hSyn promoter. The orientation and sequence were validated using Sanger sequencing. Empty
589 plasmid expressing eGFP only was used as control. These vectors were used to generate AAV serotype 2
590 at the University of Maryland virus vector core. Viral vector placement and expression were confirmed in
591 vivo by a GFP fluorescent flashlight and qPCR.

592

593 *RNA extraction, RT, and qPCR:* Total RNA was isolated and purified with RNeasy Micro Kit
594 (Qiagen), using QIAzol as a lysis reagent, including DNase treatment. All samples were tested for
595 concentration and purity using a NanoDrop (Thermo Fisher). RNA amount was normalized across samples
596 (400ng), and cDNA was created using iScript (Bio-Rad). Real-time PCR reactions were run in triplicate
597 using PowerUp SYBR Master Mix (Applied Biosystems) in a QuantStudio 7 (Thermo Fisher) qPCR
598 machine. Primer sequences: LINC00473: forward: GCATACTTTGGCGGACCTTTT, reverse
599 TGTGCCTCCCTGTGAATTCTC; HPRT1 forward: GCAGTACAGCCCCAAAATGG, reverse:
600 GGTCCTTTTCACCAGCAAGCT; GFP forward: CATGCCCGAAGGCTACGT, reverse
601 CGATGCCCTTCAGCTCGAT. Raw Ct values are presented and not normalized amounts, as LINC00473
602 is not endogenously expressed in mice.

603

604 *Virus surgery:* Mice were anesthetized by intraperitoneal injection with a mixture of Ketamine HCl
605 (100 mg/kg) and Xylazine (10 mg/kg) and positioned on a stereotaxic instrument (David Kopf Instruments).
606 In the medial prefrontal cortex (mPFC, from bregma with an angle of 15 degrees: AP +1.8 mm; ML ±0.75
607 mm; DV −2.7 mm), 0.7 µL of virus (AAV2-hSyn-GFP or AAV2-hSyn-LINC00473-GFP) was bilaterally
608 infused using 33-Gauge Hamilton needles over 5 min at a rate of 0.1 µL/min, and the needle was left in
609 place for 10-15 min after the injection before retraction. Mice were allotted 2 weeks to recover before
610 beginning food restriction across 3-4 days in preparation for testing on Restaurant Row. An initial virus
611 validation cohort (independent cohort of n=10 mice) was injected with GFP or LINC00473 viruses bilaterally
612 in mPFC at a titer of $1x10^{12}$ at. These animals were tested on Restaurant Row for only 1 week (offers
613 remained at 1 s only, first epoch, green) after which they were sacrificed for PCR validation on tissue
614 punches obtained from mPFC. Behavioral data from these animals on the conditioned-place preference
615 probe (days 0 and 8) appear in **Supplementary Fig. 4**. A second replication cohort (n=40 mice) was
616 injected with GFP or LINC00473 viruses bilaterally in mPFC at a titer of $5x10^{12}$ and served as the primary
617 cohort of animals for the main figures that underwent the full 45-day longitudinal behavioral testing. Brain
618 tissue used for immunofluorescence histological visualization of virus transfection was collected in a
619 separate set of mice three weeks post-surgery. At time of collection, animals were deeply anesthetized with
620 peritoneal injections of 500 mg/kg of Fatal Plus (Vortech, Cat #9373), and intracardially perfused with 15
621 mL 4% PFA (Electron Microscopy Science, Cat #15713-S). Brains were postfixed for 24-72 hr, and
622 subsequently sliced on a Leica VT1000 S vibratome at 40-60 µM sections. Sections were blocked for 1 hr
623 in blocking buffer (10% donkey serum (Jackson Immunoresearch, Cat #017-000-121), 0.3% Triton-X
624 (Sigma, Cat #9284) in PBS), followed by overnight incubation with primary antibody (1:1000 Ch-NeuN,
625 MilliporeSigma, Cat #ABN91) in diluted blocking buffer (1:3 dilution in PBS). Sections were washed three
626 times with diluted blocking buffer (15 min each) before incubation with secondary antibodies (Ch-647:
627 Jackson Immunoresearch, Cat# 703-605-155) for 1 hr. Two additional 15-min washes in diluted blocking
628 buffer and one 15-min wash in PBS. Finally, sections were incubated with 1:10,000 DAPI (Thermofisher,
629 Cat #62248) for 5 min. Sections were mounted with EcoMount (Biocare Medical, Cat #EM897L). Images
630 were acquired on a Zeiss LSM 900 confocal microscope using Zen Blue software with 10x and 40x oil
631 immersion lens at 1:1 digital zoom.

632

633 *Neuroeconomic Task:* Following surgery, we characterized mice longitudinally in Restaurant Row
634 [5]. On this task, mice had a limited time period each day to forage for food by navigating a maze with four
635 uniquely flavored (chocolate, banana, grape, and plain) and contextualized (horizontal stripes, dots,
636 triangles, vertical stripes) feeding sites, or "restaurants" (Fig. 1b). Animals were allotted 30 min to forage
637 for their primary source of food for the day. Rewards used on this task were obtained from BioServe (20
638 mg pellets #F007120). These pellets are full nutrition and not sucrose-only pellets that only differed in
639 flavoring but not nutritional profile (3.6 kcal/gm calories, 59.1% carbohydrate, 18.7% protein, 6.5% ash,
640 5.6% fat, 4.7% fiber). Choices on this task were interdependent across trials and across days. This makes
641 the task economic in nature, requiring animals to budget their limited time effectively in a self-paced manner
642 in order to earn a sufficient amount of food in a closed-economy system. The cost of earning a reward took
643 place in the form of a delay animals would have to wait cued by the pitch of a tone that sounded upon entry
644 into each restaurant. Each restaurant had a separate offer zone (OZ) and wait zone (WZ). Upon entry into
645 the OZ, a tone (500 ms) sounded whose pitch indicated how long of a delay mice would have to wait in a
646 cued countdown should they enter the WZ. Mice could decide to skip an offer presented in the OZ and
647 proceed down the hallway to the next restaurant. In the OZ, tones repeated every second held at the same
648 pitch to repeatedly cue the offer of the current trial until mice either made a skip or enter decision. If mice
649 decide instead to enter the WZ, this triggered a countdown with descending tone pitch stepping every
650 second until mice either waited out the full delay and earned a food pellet or quit prematurely during the
651 countdown. If mice made a skip or quit decision, the tone terminated, the offer was rescinded, and mice
652 must proceed forward to the next restaurant. Mice quickly learned to only travel in one direction as animals
653 must encounter offers serially navigating the maze in a counterclockwise direction (i.e., nothing happens if
654 mice traverse in the wrong direction other than wasting time). Mice were tested across 45 consecutive days
655 for the main experiment where strategies developed longitudinally as animals learned the structure of the
656 task and the changing economic landscape.

657

658 During the first week of testing (block 1, green epoch), all trials consisted of 1 s offers only. 1 s
659 offers were indicated by tones played at the 4,000 Hz pitch. A special probe session was inserted into this

660 timeline immediately before (day 0) and after (day 8) the first week of testing during which mice essentially
661 were allowed to roam the empty maze arena freely without any task components (no tones, no rewards) to
662 examine conditioned place preference behaviors learned through the natural experience of the first week
663 of the task itself. The remainder of the experimental timeline continued thereafter. During the next 5 days
664 of testing (block 2, yellow epoch), offers ranged from 1 to 5 s (4,000 Hz to 5,548 Hz in 387 Hz steps)
665 randomly selected from a uniform distribution. For instance, if a 4 s offer was selected on a given trial, the
666 tone presented in the OZ would be 5,161 Hz for 500 ms, and this would repeat every second indefinitely
667 until a skip or enter decision was made. If the WZ was entered, using this example trial, this 5,161 Hz tone
668 would step down by 387 Hz every second descending in pitch until earning (with the final tone of 4,000 Hz)
669 or quitting prematurely. Block 3 (5 days, orange epoch) consisted of a 1 to 15 s (4,000–9,418 Hz) range.
670 The fourth and final block (red epoch) consisted of offers ranging from 1 to 30 s (4,000–15,223 Hz) and
671 continued for the remainder of the experiment. This block-wise protocol allowed us to examine how mice
672 initially shaped their behavior as they learned the basic structure of the task as well as how they adjusted
673 their foraging strategies across long timescales (days, weeks, and months) as they transitioned from
674 reward-rich to reward-scarce environments in a stepwise manner. That is, blocks 1-3 are relatively reward
675 rich as costs are generally low delays and rewards are easier to earn compared to block 4 which is relatively
676 reward scarce as there are far more expensive reward offers distributed in the environment for which
677 animals must learn to forage efficiently. The rewards used in this task only differ in flavor for which animals
678 have subjective differences in preferences quantified below. All flavor options become increasingly scarce,
679 equally across the longitudinal paradigm.
680
681 Rewards were delivered using a custom-built 3D-printed automated pellet dispenser that was
682 triggered by a computer running the task programmed in ANY-Maze (Stoelting), run under dim lighting. The
683 task was run by video-tracking animal position in real-time where all choice contingencies are determined
684 by the centroid of the animal's body crossing territories in the maze in combination with being required to
685 run in a counterclockwise direction. The key zones in the maze include each restaurant's separate OZ and
686 WZ as well as the hallways in between restaurants (thus, 12 total main zones). 6 key behavioral epochs
687 make up all possible, mutually exclusive behaviors animals could be engaged in while spending their limited

688 time budget. 1) **Enter time**: defined from OZ entry in the correct heading direction (counterclockwise around
689 the maze) triggering tone onset until the animal physically enters right into the WZ triggering tone
690 countdown. 2) **Skip time**: defined from OZ entry in the correct heading direction triggering tone onset until
691 the animal physically exits left into the hallway. 3) **Quit time**: defined from WZ entry and tone countdown
692 onset until the animal physically exits the WZ prematurely before the countdown completes, rescinding the
693 offer and terminating the countdown. 4) **Earn time**: defined from WZ entry and tone countdown onset until
694 the countdown completes and a pellet is delivered. 5) **Consumption time**: defined from reward delivery
695 onset until the animal physically leaves the reward site and exits the WZ. 6) **Travel time**: defined from
696 previous trial termination (either from a skip, quit, or consumption event as defined above) and hallway
697 entry until the next trial begins, triggered by OZ entry into the next restaurant.
698
699 Body weight was measured twice daily, immediately before and after testing on the Restaurant
700 Row task.
701
702 *Data analysis*: In addition to simple behavioral metrics like rewards earned, laps run, reaction times
703 as described above, a key neuroeconomic behavioral metric is decision thresholds. This metric
704 approximates indifference points in choices made either in the OZ or WZ as a function of cost and flavor.
705 We measured the inflection point of fitting Heaviside step regressions to enter versus skip choices in the
706 OZ or earn versus quit choices in the WZ as a function of cued offer cost in each restaurant. Thresholds
707 determined this way were used for several subsequent analyses, including calculating reward value. The
708 value of an offer can be calculated by subtracting a trial's offer from one's WZ threshold as this reflects the
709 relative cost normalized to each animals' willingness to wait and earn a reward (i.e., offer value <0 indicate
710 offers typically not earned and thus should be skipped in the OZ or quit in the WZ as determined by each
711 animal's subjective flavor-specific decision policy which remained relatively stable across block 4 of testing).
712 Similarly, when quitting in the WZ, the value left at the moment of quitting can be calculated by subtracting
713 the time remaining in that trial's countdown from the WZ threshold (i.e., value left <0 indicates an amount
714 of time left that is not worth waiting for and should have been quit whereas value left >0 would have been
715 more advantageous to finish waiting at that point instead of quitting). The amount of time spent remaining

716 in the countdown at the moment of quitting relative to what the starting offer was and how much time was
717 spent also served as the basis of our analysis of sensitivity to sunk costs, as previously published in mice,
718 rats, and humas whereby time spent waiting can decrease the probability of quitting independent of time
719 left in the countdown, see Sweis et al *Science* for the development of this analysis [16,18,54,56,60]. Importantly,
720 this analysis depends on a control analysis that iteratively re-calculates the probability of earning a reward
721 as a function of time left remaining in the countdown from the 0 s sunk condition (see **Supplementary Fig.**
722 **8** for a graphical illustration of this control analysis). This allows all sunk cost metrics to be simplified into a
723 delta score or change in likelihood of continuing to stay, or an escalation of commitment, due purely to the
724 amount of time already spent waiting, independent of temporal distance to the goal, that controls for
725 individual differences in one's general willingness to wait or level of patience. Thresholds as well as
726 economic choice history serve as the basis and criteria used in regret-related analysis whereby distinct
727 violation vs. non-violation sequences are compared head-to-head in order to quantify the effects of mistake
728 history on influencing choice behavior on the next trial. See Steiner and Redish 2014 *Nature Neuroscience*
729 [17], Sweis et al 2018 *PLoS Biology* [5], and Durand-de Cuttoli 2022 *Science Advances* [16] for the development
730 and full description of these analyses.
731
732 Thresholds were also used for an analysis we recently developed to capture how mice develop
733 strategies that optimize food yield while also maximizing subjective value, see Durand-de Cuttoli et al 2023
734 *Biological Psychiatry* [43] for the development of this analysis. In brief, we calculated the Euclidean distance
735 between the coordinates of observed thresholds and theoretical thresholds that would yield maximal food
736 (empirically determined via simulations) versus maximal subjective value (calculated mouse-by-mouse
737 based on revealed preferences determined on day 7 projected across the remainder of testing) on each
738 day from days 18 to 45 during the 1-30 s epoch, calculated separately in both the offer zone and wait zone.
739 We ran a computer Restaurant Row simulation in order to calculate the total number of pellets earned when
740 varying different behavioral parameters. We determined that the ideal threshold required to obtain the
741 theoretical maximum number of pellets when ignoring flavor preferences was empirically determined to be
742 10 s in all restaurants and all zones when tested in a 1-30 s offer range environment. In order to determine
743 the thresholds that could yield the maximal amount of subjective value, we calculated the ratio of pellets

earned on day 7 when all offers were 1s only on a mouse-by-mouse basis. When then multiplied the theoretical food earnings output from our simulation by this mouse-specific ratio in order to transform threshold by food output into a high dimensional subjective value space. From this we could extract what combination of thresholds in all 4 restaurants when tested in a 1-30 s environment could theoretically yield the greatest amount of subjective value for each mouse. From these two sets of theoretical threshold sets (for maximal food or subjective value) we could calculate the Euclidean distance from each animal's actual observed thresholds on each day from either theoretical maximum.

Data were processed in Matlab with statistical analyses in JMP Pro 17. All data are expressed as mean ± 1 standard error. Statistical significance was assessed using student's t tests, sign tests, and one-way, two-way, three-way, and repeated measures ANOVAs. No data were excluded as outliers.

References

1 Stone, C., Mattingley, J. B. & Rangelov, D. On second thoughts: changes of mind in decision-making. *Trends Cogn Sci* **26**, 419-431 (2022).

2 Liu, X., Hairston, J., Schrier, M. & Fan, J. Common and distinct networks underlying reward valence and processing stages: a meta-analysis of functional neuroimaging studies. *Neurosci Biobehav Rev* **35**, 1219-1236 (2011). https://doi.org:10.1016/j.neubiorev.2010.12.012

3 Redish, A. D. *The mind within the brain: How we make decisions and how those decisions go wrong.*, (Oxford University Press., 2013).

4 McGuire, J. T. & Kable, J. W. Medial prefrontal cortical activity reflects dynamic re-evaluation during voluntary persistence. *Nat Neurosci* **18**, 760-766 (2015). https://doi.org:10.1038/nn.3994

5 Sweis, B. M., Thomas, M. J. & Redish, A. D. Mice learn to avoid regret. *PLoS Biol* **16**, e2005853 (2018). https://doi.org:10.1371/journal.pbio.2005853

6 Kirkebøen, G., Vasaasen, E. & Halvor Teigen, K. Revisions and Regret: The Cost of Changing your Mind. *Journal of Behavioral Decision Making* **26**, 1-12 (2011). https://doi.org:10.1002/bdm.756

7 Brenner, C. *The mind in conflict*. (International Universities Press, 1982).

8 Baumeister, R. F., Vohs, K. D. & Tice, D. M. The Strength Model of Self-Control. *Current Directions in Psychological Science* **16**, 351-355 (2016). https://doi.org:10.1111/j.1467-8721.2007.00534.x

9 American Psychiatric Association. & American Psychiatric Association. DSM-5 Task Force. *Diagnostic and statistical manual of mental disorders : DSM-5*. 5th edn, (American Psychiatric Association, 2013).

10 Mezo, P. G. & Baker, R. M. The moderating effects of stress and rumination on depressive symptoms in women and men. *Stress Health* **28**, 333-339 (2012). https://doi.org:10.1002/smi.2417

11 Seedat, S., Scott, K. M., Angermeyer, M. C., Berglund, P., Bromet, E. J., Brugha, T. S., Demyttenaere, K., de Girolamo, G., Haro, J. M., Jin, R., Karam, E. G., Kovess-Masfety, V., Levinson, D., Medina Mora, M. E., Ono, Y., Ormel, J., Pennell, B.-E., Posada-Villa, J., Sampson, N. A., Williams, D. & Kessler, R. C. Cross-National Associations Between Gender and Mental Disorders in the World Health Organization World Mental Health Surveys. *Archives of General Psychiatry* **66** (2009). https://doi.org:10.1001/archgenpsychiatry.2009.36

12 Ferrari, A. J., Charlson, F. J., Norman, R. E., Patten, S. B., Freedman, G., Murray, C. J., Vos, T. & Whiteford, H. A. Burden of depressive disorders by country, sex, age, and year: findings from the global burden of disease study 2010. *PLoS Med* **10**, e1001547 (2013). https://doi.org:10.1371/journal.pmed.1001547

13 Marcus, S. M., Kerber, K. B., Rush, A. J., Wisniewski, S. R., Nierenberg, A., Balasubramani, G. K., Ritz, L., Kornstein, S., Young, E. A. & Trivedi, M. H. Sex differences in depression symptoms in treatment-seeking adults: confirmatory analyses from the Sequenced Treatment Alternatives to Relieve Depression study. *Compr Psychiatry* **49**, 238-246 (2008). https://doi.org:10.1016/j.comppsych.2007.06.012

14 Silverstein, B. Gender differences in the prevalence of somatic versus pure depression: a replication. *Am J Psychiatry* **159**, 1051-1052 (2002). https://doi.org:10.1176/appi.ajp.159.6.1051

15 Martin, L. A., Neighbors, H. W. & Griffith, D. M. The experience of symptoms of depression in men vs women: analysis of the National Comorbidity Survey Replication. *JAMA Psychiatry* **70**, 1100-1106 (2013). https://doi.org:10.1001/jamapsychiatry.2013.1985

16 Durand-de Cuttoli, R., Martinez-Rivera, F. J., Li, L., Minier-Toribio, A., Holt, L. M., Cathomas, F., Yasmin, F., Elhassa, S. O., Shaikh, J. F., Ahmed, S., Russo, S. J., Nestler, E. J. & Sweis, B. M. Distinct forms of regret linked to resilience versus susceptibility to stress are regulated by region-specific CREB function in mice. *Science Advances* **8**, eadd5579 (2022). https://doi.org:10.1126/sciadv.add5579

17 Steiner, A. P. & Redish, A. D. Behavioral and neurophysiological correlates of regret in rat decision-making on a neuroeconomic task. *Nat Neurosci* **17**, 995-1002 (2014). https://doi.org:10.1038/nn.3740

18 Sweis, B. M., Abram, S. V., Schmidt, B. J., Seeland, K. D., Macdonald, A. W., Thomas, M. J. & Redish, A. D. Sensitivity to "sunk costs" in mice, rats, and humans. *Science* **361**, 178-181 (2018). https://doi.org:10.1126/science.aar8644

19 Eid, R. S., Gobinath, A. R. & Galea, L. A. M. Sex differences in depression: Insights from clinical and preclinical studies. *Prog Neurobiol* **176**, 86-102 (2019). https://doi.org:10.1016/j.pneurobio.2019.01.006

20 Akil, H., Gordon, J., Hen, R., Javitch, J., Mayberg, H., McEwen, B., Meaney, M. J. & Nestler, E. J. Treatment resistant depression: A multi-scale, systems biology approach. *Neurosci Biobehav Rev* **84**, 272-288 (2018). https://doi.org:10.1016/j.neubiorev.2017.08.019

21 Ulitsky, I. & Bartel, D. P. lincRNAs: genomics, evolution, and mechanisms. *Cell* **154**, 26-46 (2013). https://doi.org:10.1016/j.cell.2013.06.020

22 Issler, O., van der Zee, Y. Y., Ramakrishnan, A., Wang, J., Tan, C., Loh, Y. E., Purushothaman, I., Walker, D. M., Lorsch, Z. S., Hamilton, P. J., Pena, C. J., Flaherty, E., Hartley, B. J., Torres-Berrio, A., Parise, E. M., Kronman, H., Duffy, J. E., Estill, M. S., Calipari, E. S., Labonte, B., Neve, R. L., Tamminga, C. A., Brennand, K. J., Dong, Y., Shen, L. & Nestler, E. J. Sex-Specific Role for the Long Non-coding RNA LINC00473 in Depression. *Neuron* **106**, 912-926 e915 (2020). https://doi.org:10.1016/j.neuron.2020.03.023

23 Chen, Z., Li, J. L., Lin, S., Cao, C., Gimbrone, N. T., Yang, R., Fu, D. A., Carper, M. B., Haura, E. B., Schabath, M. B., Lu, J., Amelio, A. L., Cress, W. D., Kaye, F. J. & Wu, L. cAMP/CREB-regulated LINC00473 marks LKB1-inactivated lung cancer and mediates tumor growth. *J Clin Invest* **126**, 2267-2279 (2016). https://doi.org:10.1172/JCI85250

24 Jiang, L. Y., Wang, G. H., Xu, J. J., Li, X. L., Lin, X. Y., Fang, X., Zhang, H. X., Feng, M. & Jiang, C. M. CREB-induced LINC00473 promotes chemoresistance to TMZ in glioblastoma by regulating O6-methylguanine-DNA-methyltransferase expression via CEBPalpha binding. *Neuropharmacology* **243**, 109790 (2024). https://doi.org:10.1016/j.neuropharm.2023.109790

25 Ataman, B., Boulting, G. L., Harmin, D. A., Yang, M. G., Baker-Salisbury, M., Yap, E. L., Malik, A. N., Mei, K., Rubin, A. A., Spiegel, I., Durresi, E., Sharma, N., Hu, L. S., Pletikos, M., Griffith, E. C., Partlow, J. N., Stevens, C. R., Adli, M., Chahrour, M., Sestan, N., Walsh, C. A., Berezovskii, V. K., Livingstone, M. S. & Greenberg, M. E. Evolution of Osteocrin as an activity-regulated factor in the primate brain. *Nature* **539**, 242-247 (2016). https://doi.org:10.1038/nature20111

26 Pruunsild, P., Bengtson, C. P., Loss, I., Lohrer, B. & Bading, H. Expression of the primate-specific LINC00473 RNA in mouse neurons promotes excitability and CREB-regulated transcription. *J Biol Chem* **299**, 104671 (2023). https://doi.org:10.1016/j.jbc.2023.104671

27 Pruunsild, P., Bengtson, C. P. & Bading, H. Networks of Cultured iPSC-Derived Neurons Reveal the Human Synaptic Activity-Regulated Adaptive Gene Program. *Cell Rep* **18**, 122-135 (2017). https://doi.org:10.1016/j.celrep.2016.12.018

28 Tran, K. V., Brown, E. L., DeSouza, T., Jespersen, N. Z., Nandrup-Bus, C., Yang, Q., Yang, Z., Desai, A., Min, S. Y., Rojas-Rodriguez, R., Lundh, M., Feizi, A., Willenbrock, H., Larsen, T. J., Severinsen, M. C. K., Malka, K., Mozzicato, A. M., Deshmukh, A. S.,

Emanuelli, B., Pedersen, B. K., Fitzgibbons, T., Scheele, C., Corvera, S. & Nielsen, S. Human thermogenic adipocyte regulation by the long noncoding RNA LINC00473. *Nat Metab* **2**, 397-412 (2020). https://doi.org:10.1038/s42255-020-0205-x

29 Barrot, M., Olivier, J. D., Perrotti, L. I., DiLeone, R. J., Berton, O., Eisch, A. J., Impey, S., Storm, D. R., Neve, R. L., Yin, J. C., Zachariou, V. & Nestler, E. J. CREB activity in the nucleus accumbens shell controls gating of behavioral responses to emotional stimuli. *Proc Natl Acad Sci U S A* **99**, 11435-11440 (2002). https://doi.org:10.1073/pnas.172091899

30 Carlezon, W. A., Jr., Duman, R. S. & Nestler, E. J. The many faces of CREB. *Trends Neurosci* **28**, 436-445 (2005). https://doi.org:10.1016/j.tins.2005.06.005

31 Kim, J., Kwon, J. T., Kim, H. S., Josselyn, S. A. & Han, J. H. Memory recall and modifications by activating neurons with elevated CREB. *Nat Neurosci* **17**, 65-72 (2014). https://doi.org:10.1038/nn.3592

32 Lonze, B. E. & Ginty, D. D. Function and regulation of CREB family transcription factors in the nervous system. *Neuron* **35**, 605-623 (2002). https://doi.org:10.1016/s0896-6273(02)00828-0

33 McClung, C. A. & Nestler, E. J. Regulation of gene expression and cocaine reward by CREB and DeltaFosB. *Nat Neurosci* **6**, 1208-1215 (2003). https://doi.org:10.1038/nn1143

34 Sakai, N., Thome, J., Newton, S. S., Chen, J., Kelz, M. B., Steffen, C., Nestler, E. J. & Duman, R. S. Inducible and brain region-specific CREB transgenic mice. *Mol Pharmacol* **61**, 1453-1464 (2002). https://doi.org:10.1124/mol.61.6.1453

35 Lorsch, Z. S., Hamilton, P. J., Ramakrishnan, A., Parise, E. M., Salery, M., Wright, W. J., Lepack, A. E., Mews, P., Issler, O., McKenzie, A., Zhou, X., Parise, L. F., Pirpinias, S. T., Ortiz Torres, I., Kronman, H. G., Montgomery, S. E., Loh, Y. E., Labonte, B., Conkey, A., Symonds, A. E., Neve, R. L., Turecki, G., Maze, I., Dong, Y., Zhang, B., Shen, L., Bagot, R. C. & Nestler, E. J. Stress resilience is promoted by a Zfp189-driven transcriptional network in prefrontal cortex. *Nat Neurosci* **22**, 1413-1423 (2019). https://doi.org:10.1038/s41593-019-0462-8

36 Glimcher, P. W. & Rustichini, A. Neuroeconomics: the consilience of brain and decision. *Science* **306**, 447-452 (2004). https://doi.org:10.1126/science.1102566

37 Kenning, P. & Plassmann, H. Neuroeconomics: an overview from an economic perspective. *Brain Res Bull* **67**, 343-354 (2005). https://doi.org:10.1016/j.brainresbull.2005.07.006

38 Loewenstein, G., Rick, S. & Cohen, J. D. Neuroeconomics. *Annu Rev Psychol* **59**, 647-672 (2008). https://doi.org:10.1146/annurev.psych.59.103006.093710

39 Kalenscher, T. & Pennartz, C. M. Is a bird in the hand worth two in the future? The neuroeconomics of intertemporal decision-making. *Prog Neurobiol* **84**, 284-315 (2008). https://doi.org:10.1016/j.pneurobio.2007.11.004

40 Clithero, J. A. & Rangel, A. Informatic parcellation of the network involved in the computation of subjective value. *Soc Cogn Affect Neurosci* **9**, 1289-1302 (2014). https://doi.org:10.1093/scan/nst106

41 Levy, D. J. & Glimcher, P. W. The root of all value: a neural common currency for choice. *Curr Opin Neurobiol* **22**, 1027-1038 (2012). https://doi.org:10.1016/j.conb.2012.06.001

42 Louie, K. & Glimcher, P. W. Efficient coding and the neural representation of value. *Ann N Y Acad Sci* **1251**, 13-32 (2012). https://doi.org:10.1111/j.1749-6632.2012.06496.x

43 Durand-de Cuttoli, R., Martinez-Rivera, F. J., Li, L., Minier-Toribio, A., Dong, Z., Cai, D. J., Russo, S. J., Nestler, E. J. & Sweis, B. M. A double-hit of social and economic stress in mice precipitates changes in decision-making strategies. *Biol Psychiatry* (2023). https://doi.org:10.1016/j.biopsych.2023.12.011

44 Resulaj, A., Kiani, R., Wolpert, D. M. & Shadlen, M. N. Changes of mind in decision-making. *Nature* **461**, 263-266 (2009). https://doi.org:10.1038/nature08275

45 Hare, T. A., Camerer, C. F. & Rangel, A. Self-control in decision-making involves modulation of the vmPFC valuation system. *Science* **324**, 646-648 (2009). https://doi.org:10.1126/science.1168450

46 Alagapan, S., Choi, K. S., Heisig, S., Riva-Posse, P., Crowell, A., Tiruvadi, V., Obatusin, M., Veerakumar, A., Waters, A. C., Gross, R. E., Quinn, S., Denison, L., O'Shaughnessy, M., Connor, M., Canal, G., Cha, J., Hershenberg, R., Nauvel, T., Isbaine, F., Afzal, M. F., Figee, M., Kopell, B. H., Butera, R., Mayberg, H. S. & Rozell, C. J. Cingulate dynamics track depression recovery with deep brain stimulation. *Nature* **622**, 130-138 (2023). https://doi.org:10.1038/s41586-023-06541-3

47 Knutson, B., Bhanji, J. P., Cooney, R. E., Atlas, L. Y. & Gotlib, I. H. Neural responses to monetary incentives in major depression. *Biol Psychiatry* **63**, 686-692 (2008). https://doi.org:10.1016/j.biopsych.2007.07.023

48 Holton, E., Grohn, J., Ward, H., Manohar, S. G., O'Reilly, J. X. & Kolling, N. Goal commitment is supported by vmPFC through selective attention. *Nature Human Behaviour* (2024). https://doi.org:10.1038/s41562-024-01844-5

49 Sweis, B. M. & Nestler, E. J. Pushing the boundaries of behavioral analysis could aid psychiatric drug discovery. *PLoS Biol* **20**, e3001904 (2022). https://doi.org:10.1371/journal.pbio.3001904

50 Sweis, B. M., Thomas, M. J. & Redish, A. D. Beyond simple tests of value: measuring addiction as a heterogeneous disease of computation-specific valuation processes. *Learn Mem* **25**, 501-512 (2018). https://doi.org:10.1101/lm.047795.118

51 Abram, S. V., Breton, Y. A., Schmidt, B., Redish, A. D. & MacDonald, A. W., 3rd. The Web-Surf Task: A translational model of human decision-making. *Cogn Affect Behav Neurosci* **16**, 37-50 (2016). https://doi.org:10.3758/s13415-015-0379-y

52 Maisson, D., Voloh, B., Cervera, R., Conover, I., Zambre, M., Zimmermann, J. & Hayden, B. Widespread coding of navigational variables in prefrontal cortex *biorxiv* (2022). https://doi.org:10.1101/2022.10.13.512139

53 McInnes, A. N., Sullivan, C. R. P., III, A. W. M. & Widge, A. S. Psychometric validation and clinical correlates of an experiential foraging task. *BioRxiv* **2023.12.28.573439** (2023).

54 Kazinka, R., MacDonald, A. W., 3rd & Redish, A. D. Sensitivity to Sunk Costs Depends on Attention to the Delay. *Front Psychol* **12**, 604843 (2021). https://doi.org:10.3389/fpsyg.2021.604843

55 Abram, S. V., Hanke, M., Redish, A. D. & MacDonald, A. W., 3rd. Neural signatures underlying deliberation in human foraging decisions. *Cogn Affect Behav Neurosci* **19**, 1492-1508 (2019). https://doi.org:10.3758/s13415-019-00733-z

56 Redish, A. D., Abram, S. V., Cunningham, P. J., Duin, A. A., Durand-de Cuttoli, R., Kazinka, R., Kocharian, A., MacDonald, A. W., 3rd, Schmidt, B., Schmitzer-Torbert, N., Thomas, M. J. & Sweis, B. M. Sunk cost sensitivity during change-of-mind decisions is informed by both the spent and remaining costs. *Commun Biol* **5**, 1337 (2022). https://doi.org:10.1038/s42003-022-04235-6

57 Sweis, B. M., Larson, E. B., Redish, A. D. & Thomas, M. J. Altering gain of the infralimbic-to-accumbens shell circuit alters economically dissociable decision-making algorithms. *Proc Natl Acad Sci U S A* **115**, E6347-E6355 (2018). https://doi.org:10.1073/pnas.1803084115

58 Sweis, B. M., Redish, A. D. & Thomas, M. J. Prolonged abstinence from cocaine or morphine disrupts separable valuations during decision conflict. *Nat Commun* **9**, 2521 (2018). https://doi.org:10.1038/s41467-018-04967-2

59 Diehl, G. & Redish, A. D. Differential processing of decision information in subregions of rodent medial prefrontal cortex. *biorxiv* (2022).

60 Duin, A. A., Aman, L., Schmidt, B. & Redish, A. D. Certainty and uncertainty of the future changes planning and sunk costs. *Behav Neurosci* (2021). https://doi.org:10.1037/bne0000460

61 Schmidt, B., Duin, A. A. & Redish, A. D. Disrupting the medial prefrontal cortex alters hippocampal sequences during deliberative decision making. *J Neurophysiol* **121**, 1981-2000 (2019). https://doi.org:10.1152/jn.00793.2018

62 Schmidt, B. & Redish, A. D. Disrupting the medial prefrontal cortex with designer receptors exclusively activated by designer drug alters hippocampal sharp-wave ripples and their associated cognitive processes. *Hippocampus* (2021). https://doi.org:10.1002/hipo.23367

63 Nwakama, C. A., Durand-de Cuttoli, R., Oketokoun, Z. M., Brown, S. O., Haller, J. E., Mendez, A., Farshbaf, M. J., Cho, Y. Z., Ahmed, S., Leng, S., Ables, J. L. & Sweis, B. M. Diabetes alters neuroeconomically dissociable forms of mental accounting. *bioRxiv* (2024). https://doi.org:doi.org/10.1101/2024.01.04.574210

64 Kocharian, A., Redish, A. D. & Rothwell, P. E. Individual differences in decision-making shape how mesolimbic dopamine regulates choice confidence and change-of-mind. *bioRxiv* (2024). https://doi.org:10.1101/2024.09.16.613237

65 German, P. W. & Fields, H. L. Rat nucleus accumbens neurons persistently encode locations associated with morphine reward. *J Neurophysiol* **97**, 2094-2106 (2007). https://doi.org:10.1152/jn.00304.2006

66 Sjulson, L., Peyrache, A., Cumpelik, A., Cassataro, D. & Buzsaki, G. Cocaine Place Conditioning Strengthens Location-Specific Hippocampal Coupling to the Nucleus Accumbens. *Neuron* **98**, 926-934 e925 (2018). https://doi.org:10.1016/j.neuron.2018.04.015

67 Bardo, M. T. & Bevins, R. A. Conditioned place preference: what does it add to our preclinical understanding of drug reward? *Psychopharmacology* **153**, 31-43 (2000). https://doi.org:10.1007/s002130000569

68 Tzschentke, T. M. Measuring reward with the conditioned place preference (CPP) paradigm: update of the last decade. *Addict Biol* **12**, 227-462 (2007). https://doi.org:10.1111/j.1369-1600.2007.00070.x

69 Johnson, A. & Redish, A. D. Neural ensembles in CA3 transiently encode paths forward of the animal at a decision point. *J Neurosci* **27**, 12176-12189 (2007). https://doi.org:10.1523/JNEUROSCI.3761-07.2007

70 Kay, K., Chung, J. E., Sosa, M., Schor, J. S., Karlsson, M. P., Larkin, M. C., Liu, D. F. & Frank, L. M. Constant Sub-second Cycling between Representations of Possible Futures in the Hippocampus. *Cell* **180**, 552-567 e525 (2020). https://doi.org:10.1016/j.cell.2020.01.014

71 Huynh, T., Alstatt, K., Abram, S. V. & Schmitzer-Torbert, N. Vicarious Trial-and-Error Is Enhanced During Deliberation in Human Virtual Navigation in a Translational Foraging Task. *Front Behav Neurosci* **15**, 586159 (2021). https://doi.org:10.3389/fnbeh.2021.586159

72 Diehl, G. & Redish, A. D. Measuring excitation-inhibition balance through spectral components of local field potentials. *bioRxiv* (2024). https://doi.org:doi.org/10.1101/2024.01.24.577086

73 Redish, A. D. Vicarious trial and error. *Nat Rev Neurosci* **17**, 147-159 (2016). https://doi.org:10.1038/nrn.2015.30

74 Lind, E. B., Sweis, B. M., Asp, A. J., Esguerra, M., Silvis, K. A., David Redish, A. & Thomas, M. J. A quadruple dissociation of reward-related behaviour in mice across excitatory inputs to the nucleus accumbens shell. *Commun Biol* **6**, 119 (2023). https://doi.org:10.1038/s42003-023-04429-6

75 Ressler, K. J. & Mayberg, H. S. Targeting abnormal neural circuits in mood and anxiety disorders: from the laboratory to the clinic. *Nat Neurosci* **10**, 1116-1124 (2007). https://doi.org:10.1038/nn1944

76 Durand-de Cuttoli, R., Martinez-Rivera, F. J., Li, L., Minier-Toribio, A., Russo, S. J., Nestler, E. J. & Sweis, B. M. Chronic social stress induces isolated deficits in reward anticipation on a neuroeconomic foraging task. *biorxiv* (2022). https://doi.org:10.1101/2022.01.17.476514

77 Barrot, M., Wallace, D. L., Bolanos, C. A., Graham, D. L., Perrotti, L. I., Neve, R. L., Chambliss, H., Yin, J. C. & Nestler, E. J. Regulation of anxiety and initiation of sexual behavior by CREB in the nucleus accumbens. *Proc Natl Acad Sci U S A* **102**, 8357-8362 (2005). https://doi.org:10.1073/pnas.0500587102

78 Dong, Y., Green, T., Saal, D., Marie, H., Neve, R., Nestler, E. J. & Malenka, R. C. CREB modulates excitability of nucleus accumbens neurons. *Nat Neurosci* **9**, 475-477 (2006). https://doi.org:10.1038/nn1661

79 Zhou, J., Zhang, H., Cohen, R. S. & Pandey, S. C. Effects of Estrogen Treatment on Expression of Brain-Derived Neurotrophic Factor and cAMP Response Element-Binding Protein Expression and Phosphorylation in Rat Amygdaloid and Hippocampal Structures. *Neuroendocrinology* **81**, 294-310 (2005). https://doi.org:10.1159/000088448

80 Sharma, K., Mehra, R. D., Dhar, P. & Vij, U. Chronic exposure to estrogen and tamoxifen regulates synaptophysin and phosphorylated cAMP response element-binding (CREB) protein expression in CA1 of ovariectomized rat hippocampus. *Brain Res* **1132**, 10-19 (2007). https://doi.org:10.1016/j.brainres.2006.11.027

81 Lorsch, Z. S., Loh, Y. E., Purushothaman, I., Walker, D. M., Parise, E. M., Salery, M., Cahill, M. E., Hodes, G. E., Pfau, M. L., Kronman, H., Hamilton, P. J., Issler, O., Labonte, B., Symonds, A. E., Zucker, M., Zhang, T. Y., Meaney, M. J., Russo, S. J., Shen, L., Bagot, R. C. & Nestler, E. J. Estrogen receptor alpha drives pro-resilient transcription in mouse models of depression. *Nat Commun* **9**, 1116 (2018). https://doi.org:10.1038/s41467-018-03567-4

82 Shansky, R. M., Glavis-Bloom, C., Lerman, D., McRae, P., Benson, C., Miller, K., Cosand, L., Horvath, T. L. & Arnsten, A. F. Estrogen mediates sex differences in stress-induced prefrontal cortex dysfunction. *Mol Psychiatry* **9**, 531-538 (2004). https://doi.org:10.1038/sj.mp.4001435

83 Issler, O., van der Zee, Y. Y., Ramakrishnan, A., Xia, S., Zinsmaier, A. K., Tan, C., Li, W., Browne, C. J., Walker, D. M., Salery, M., Torres-Berrío, A., Futamura, R., Duffy, J. E., Labonte, B., Girgenti, M. J., Tamminga, C. A., Dupree, J. L., Dong, Y., Murrough, J. W., Shen, L. & Nestler, E. J. The long noncoding RNA FEDORA is a cell type– and sex-specific regulator of depression. *Science Advances* **8** (2022). https://doi.org:10.1126/sciadv.abn9494

Acknowledgments:

We thank Pete Rudebeck and members of the labs of Eric Nestler and Scott Russo for helpful discussion and technical assistance. Open-source illustrations obtained from SciDraw (www.scidraw.io), credit Federico Claudi and Annie Park.

Funding:

National Institute of Mental Health grant R01MH136230 (BMS)
National Institute of Mental Health grant R01MH051399 (EJN)
National Institute of Mental Health grant R01MH129306 (EJN)
National Institute of Mental Health grant R01MH114882 (SJR)
National Institute of Mental Health grant R01MH127820 (SJR)
National Institute of Mental Health grant R01MH104559 (SJR)
National Institute of Mental Health grant L40MH127601 (BMS)
National Institute of Mental Health training grant R25MH129256 (BMS)
National Institute of Mental Health supplement grant R01MH051399-31S1 (BMS)
Leon Levy Scholarship in Neuroscience, New York Academy of Sciences (BMS)
Burroughs Wellcome Fund Career Award for Medical Scientists (BMS)
Animal Models for the Social Dimensions of Health and Aging Research Network via NIH/NIA R24 AG065172 (BMS)
Brain & Behavior Research Foundation NARSAD Young Investigator Award 32856 (BMS)
Brain & Behavior Research Foundation NARSAD Young Investigator Award 31140 (RDC)

Author contributions:

Conceptualization: RDC, OI, EJN, BMS
Methodology: RDC, OI, BMS

Investigation: RDC, OI, SMBP, BY, NJ, AA, SK, KG, SA, SJR, EJN, BMS

Data curation: RDC, OI, BMS

Formal analysis: BMS

Visualization: RDC, OI, SMBP, BMS

Funding acquisition: OI, BMS

Supervision: RDC, BMS

Writing – original draft: RDC, OI, SMBP, BMS

Writing – review & editing: RDC, OI, SBMP, BY, NJ, AA, SK, KG, SA, SJR, EJN, BMS

Competing interests:

Authors declare that they have no competing interests.

Data and materials availability:

All data and materials used in the analysis are available in the manuscript, materials and methods section, or supplementary information.

1088 **Figure Captions:**

1089

1090 **Fig. 1 | Male and female mice similarly acquire the Restaurant Row task. a** Timeline. Representative
1091 images of surgical targeting and virus transfection of GFP at 40x and 10x magnifications with DAPI and
1092 NeuN staining. Mice were allowed to recover before beginning longitudinal testing on the Restaurant Row
1093 task for 45 consecutive days. Dashed box indicates time period relevant for this figure: week 1 of testing. **b**
1094 Task schematic. Mice were allotted 30 min daily to invest time foraging for their primary source of food in a
1095 self-paced manner. Costs to obtain rewards were in the form of delays mice would have to wait near feeder
1096 sites. Mice were required to run in a counterclockwise direction encountering offers for different flavors at
1097 each "restaurant" in serial order. Each restaurant, separated by hallways, was divided into a T-shaped "offer
1098 zone" choice point and a separate "wait zone" that housed the pellet dispenser. Upon offer zone entry from
1099 the correct heading-direction, a tone sounded whose pitch indicated the delay mice would have to wait if
1100 accepting the offer by entering the wait zone. If entered, tone pitch descended in the wait zone, cuing the
1101 indicated delay. Each trial terminated if mice skipped in the offer zone, quit during the countdown in the
1102 wait zone, or earned a reward, after which animals were required to proceed to the next restaurant. **c-f**
1103 Behavioral metrics across the first week of testing during which all offers were 1 s only (lowest pitch, 4 kHz):
1104 (c) distance traveled, (d) laps run in the correct direction, (e) rewards earned, (f) earnings split by flavors
1105 ranked from least to most preferred by summing each day's end-of-session totals in each restaurant. No
1106 effect of sex or LINC00473 expression was grossly apparent in these initial metrics. Error bars represent
1107 ±1 SEM.

1108

1109 **Fig. 2 | LINC00473 expression in mPFC alters sex- and value-dependent, task-driven conditioned**
1110 **place preference behavior. a** Timeline. Dashed box indicates time period relevant for this figure: two
1111 special testing days marked with cyan arrows. **b** Experimental design. Animals were placed in the arena
1112 free to roam for 20 min on day 0 and day 8 of the experimental timeline but with no active task to obtain
1113 pre-task baseline and post-task experience-related exploratory behavior. **c** Total number of entries and
1114 total time spent in the wait zone, aggregated in all restaurants. **d-e** Representative video tracking data from
1115 an example mouse [GFP-treated female] recorded during the pre (day 0) and post (day 8) tests. (d) Track

1116 plots displaying body position when traveling between restaurants (gray) and when in the wait zone of each
1117 restaurant (colored). (e) Occupancy heat maps of the same example mouse in (d). The change in entries
1118 into and time spent in each restaurant's wait zone can be calculated as a delta score (post minus pre), color
1119 of these example heat maps is scaled across sessions to the maximum occupancy (130s). **f-g** Delta scores
1120 in change of (f) total entries and (g) total time comparing post (day 8) minus pre (day 0) time points split by
1121 restaurants ranked according to rewards earned on the active task on day 7. Only the most preferred (1st)
1122 and least preferred (4th, faint) restaurants are depicted here (see **Supplementary Fig. 4** for full dataset and
1123 replication cohort). Horizontal dashed gray line indicates delta score of 0. LINC00473 expression in mPFC
1124 abolished CPP behavior in most preferred restaurants only in females and only in the time but not entry
1125 domain. *Represent significant sex differences. Error bars represent ±1 SEM.
1126
1127 **Fig. 3 | Escalating reward scarcity unmasks sex-dependent effects of LINC00473 expression in**
1128 **mPFC on complex foraging profiles. a** Timeline. Dashed box indicates time period relevant for this figure:
1129 entire 45-day Restaurant Row paradigm. **b** Rewards earned (black) and laps run in the correct direction
1130 (gray). All 40 mice. Color bars along the x-axis reflect the distribution of offers illustrated in (a). Vertical
1131 dashed green-yellow-red lines indicate transition points of the stepwise schedule and are re-used
1132 throughout all other figures as a visual aid. Inset depicts "hysteresis" plot of laps against earns (epochs of
1133 days are color-coded). **c** Rewards earned split by flavors ranked from most preferred (1st) to least preferred
1134 (4th, faint). All 40 mice. **d** Change in rewards earned in each restaurant comparing two days at various color-
1135 coded transition points (delta scores calculated by subtracting the following: i, day 8-7 (yellow); ii, day 13-
1136 12 (orange); iii, day 18-17 (red); iv, day 45-18 (purple). All 40 mice (see **Supplementary Fig. 5** for group
1137 comparisons). **e** Portion of total session time engaged in four major choice behaviors: offer zone – enter
1138 (green) or skip (red); wait zone – quit (magenta) or earn (blue). Rings split restaurants ranked from most
1139 (1st, inner ring) to least preferred (4th, outer ring). Each of the 5 pie charts represent data from each testing
1140 stage, with the early and late epochs during the 1-30 s offer range from the first 5 and last 5 days of that
1141 period. **f** Laps run in the correct direction split by sex and treatment. **g** Proportion of enter decisions
1142 terminating in a quit outcome once in the wait zone. LINC00473 expression in mPFC drove females to run

more laps in response to a worsening economic landscape and quit more frequently. *Represent significant sex differences. Shading / error bars represent ±1 SEM.

Fig. 4 | Change-of-mind decision-making patterns reveal unique sex-dependent neuroeconomic policies . a Timeline. **b** Example behavior from a single mouse during the 1-30 s epoch (early: days 18-22, late: days 41-45). Example offer zone and wait zone thresholds indicated by the vertical dashed green (oz th) and blue (wz th) lines respectively in each restaurant. **c** Summary data from all 40 mice early or late during the 1-30 s epoch. **d** Thresholds of willingness to accept offers in the offer zone or earn offers in the wait zone. Inset depicts an example session from a single mouse in one restaurant. All 40 mice. Top inset depicts "hysteresis" plot of offer zone against wait zone thresholds (epochs color-coded). **e** Offer zone thresholds (top) and wait zone thresholds (bottom) split by sex and treatment. **f** Thresholds in (e) from early and late 1-30 s epoch. **g-i** Economic analysis of how decision policies during the 1-30 s epoch approximate maximal food vs. subjective value (see **Methods** and **Supplementary Fig. 7** for full explanation). (g) Individual differences in (top) standard deviation of rewards earned across flavors on day 7, (middle) total rewards earned on day 7, and (bottom) earns split by restaurant (flavor: chocolate-brown, banana-yellow, grape-purple, plain-cyan) and size (reward count) on day 7. All data in (g) is sorted by standard deviation data in (top). Small colored boxes along the x-axis indicate sex (male-blue, female-red) and treatment (LINC-dark, GFP-light). **h** Example data from a single mouse on day 7 showing earn ratios between flavors. **i** Data from (g-h) used in a computational modeling analysis to calculate the Euclidean distance between observed and theoretical decision policies for maximal food (brown) or subjective value (magenta) separately for offer zone and wait zone thresholds. *Represent significant sex differences. Shading / error bars represent ±1 SEM.

Fig. 5 | LINC00473 expression in mPFC alters the temporal dynamics of change-of-mind decisions. a Distribution of quit trials by offer value or value left from the 1-30 s epoch. **b** Average value left at quit. **c** Three categories of quit events based on offer value and value left. **d** Number of quit events from each quit category in (c). **e** Split by restaurants ranked from least (4th) to most preferred (1st) from the 1-30 s epoch. **f-h** Sunk cost analysis of staying behavior in the wait zone. (f) Likelihood of staying in the wait zone as a

function of time left in the countdown and time already spent waiting. Black 0 s time spent represents just entering the wait zone. Inset llustrates an example analysis point matched at 10 s left. Data from (f) dimensioned reduced in (g) collapsing across time left. Insets in (g) depict data from curves in (f) collapsed into the observed (sunk condition) and control (0 s condition) lines. Difference between curves in (g) are plotted in (h) to summarize the envelope of the overall effect of time already spent on staying in the wait zone. **i** Sensitivity to sunk costs across the entire paradigm. **j-k** Regret-related sequence analyses comparing trial pairs between (j) type 1 scenarios and (k) type 2 scenarios. Read out trials captures a change in behavior depending on choice history of distinct economic violations (black) compared to non-violations (gray) on trial t-1. See **Methods** for a full explanation of these analyses. Prominent sex-dependent effect revealed by LINC00473 expression in mPFC on change-of-mind related sunk costs (enhanced in females) and regret sensitivity (type 2: enhanced in females). ***** in (b-i) represent significant sex differences. * in (j-k) represent delta score significantly different from 0. Shading / error bars represent ±1 SEM.

Fig. 6 | Summary of key findings. Distinction between decision-making processes measured within trial in the offer zone (deliberative choices between skipping vs. entering) and wait zone (re-evaluative choices between quitting vs. continuing to wait before earning a reward, star symbol) as a function of cued delay costs (tone pitch, colored notes) and subjective value (flavor). Analysis of foraging behaviors reveal signatures of dissociable neuroeconomic processes in the offer zone (willingness to enter, vicarious trial and error choice behavior, behavioral sensitivity to type 1 regret scenarios: the impact of skipping high-value offers on subsequent choices) and wait zone (willingness to wait, behavioral sensitivity to sunk costs, and behavioral sensitivity to type 2 regret scenarios: the impact of entering and then quitting low-value offers on subsequent choices). Interlocking male and female symbols (⚥) represent no sex differences while separated symbols (♀ ♂) indicate sex differences, either at baseline (GFP group) or altered by LINC00473 expression in mPFC. See **Supplementary Fig. 14** for an expanded summary table.

Fig. 7 | Conceptual neuroeconomic framework. Working model of the link between key wait zone phenotypes enhanced in LINC00473-treated females during change-of-mind decision-making. This schematic depicts the choice conflict after mice accept a high-cost offer – an economic violation in the offer

zone – once they arrive in the wait zone and are faced with competing actions to stay vs. quit. Clock emphasizes that this decision process evolves with the passage of time. Quitting rapidly is most economically advantageous. Yet, accruing sunk costs promotes staying as added value is cached over time. If these trials are quit – a defining feature of type 2 regret scenarios – this added value is carried into subsequent trials, augmenting future choices. Red arrows highlight enhanced sensitivity to sunk costs and type 2 regret apparent in LINC00473-treated females compared to baseline (gray). Sunk costs: p(stay) increases as a function of time spent waiting on trial T; Type 2 regret: p(compensate) [increased likelihood of accepting offers typically rejected on trial T+1] is higher following violation sequences [enter-then-quit] relative to non-violation control sequences [skip] for high-cost offers on trial T. Proposed unifying principle linking sensitivity to sunk costs and type 2 regret: Both phenomena stem from the same trial pool on trial T: inappropriately accepting a high-cost offer. Alterations in reward value, driving either sunk cost-induced staying or post-quit regret-related compensatory behavior, may stem from a shared value function. There may be a common underlying counterfactual process where the unselected alternative (i.e., skipping trial T instead) carries added value and influences behavior either during staying or after quitting. This value function in either case minimizes future loss. This work makes explicit predictions about hypotheses for future research investigating the neural correlates of shared counterfactual representations and, clinically, if the content of negative rumination in mood disorders maps onto these representations.

Figure 1

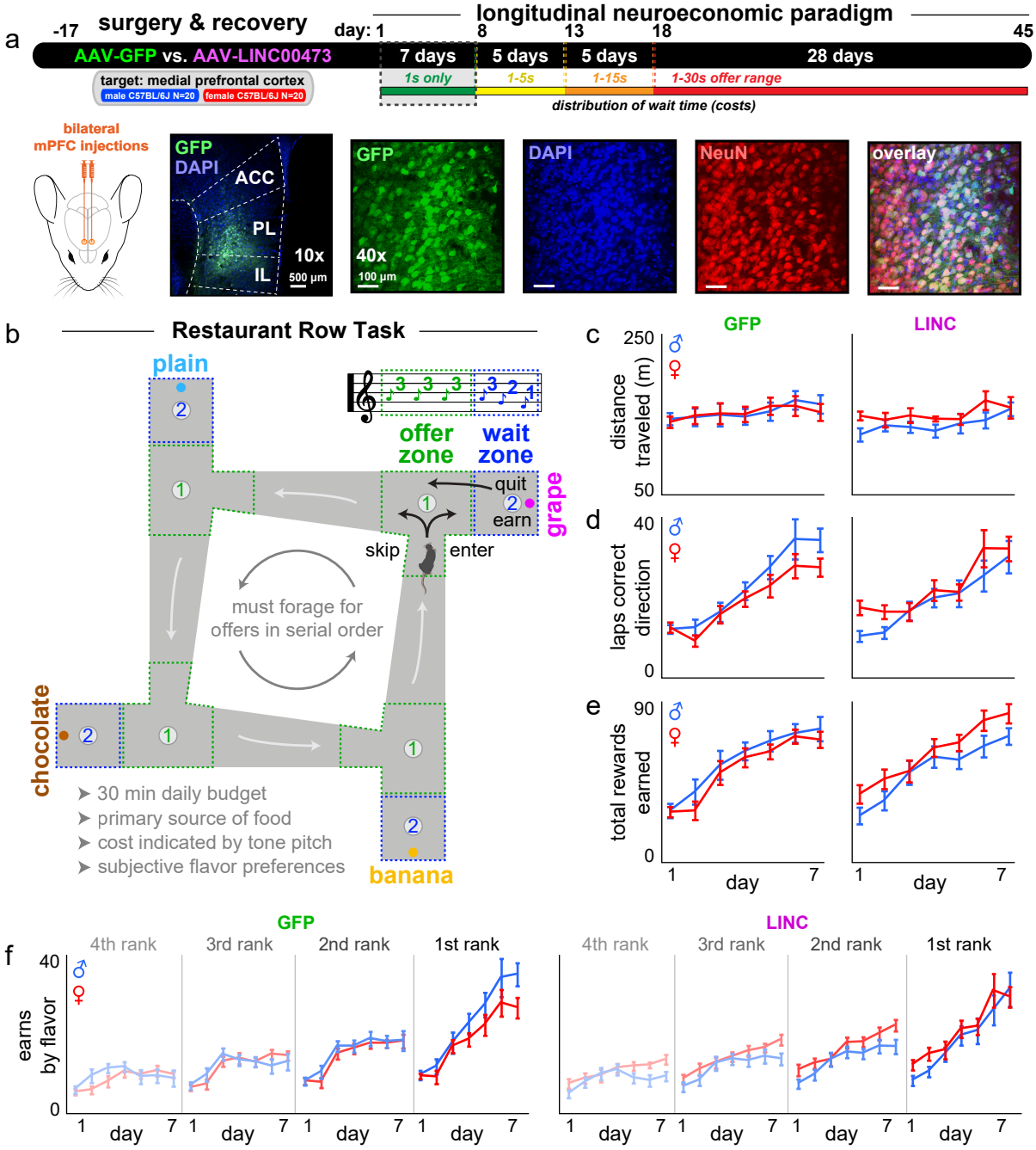
a
-17
surgery & recovery
longitudinal neuroeconomic paradigm
day: 1
8
13
18
45
AAV-GFP vs. AAV-LINC00473
7 days
5 days
5 days
28 days
target: medial prefrontal cortex
male C57BL/6J N=20
female C57BL/6J N=20
1s only
1-5s
1-15s
1-30s offer range
distribution of wait time (costs)
bilateral
mPFC injections
GFP
DAPI
ACC
PL
IL
10x
500 µm
GFP
40x
100 µm
DAPI
NeuN
overlay
b
Restaurant Row Task
plain
offer
zone
wait
zone
quit
earn
grape
skip
enter
must forage for
offers in serial order
chocolate
banana
30 min daily budget
primary source of food
cost indicated by tone pitch
subjective flavor preferences
c
GFP
LINC
distance
traveled (m)
250
50
d
laps correct
direction
40
0
e
total rewards
earned
90
0
1
day
7
f
GFP
LINC
4th rank
3rd rank
2nd rank
1st rank
earns
by flavor
40
0

Figure 2

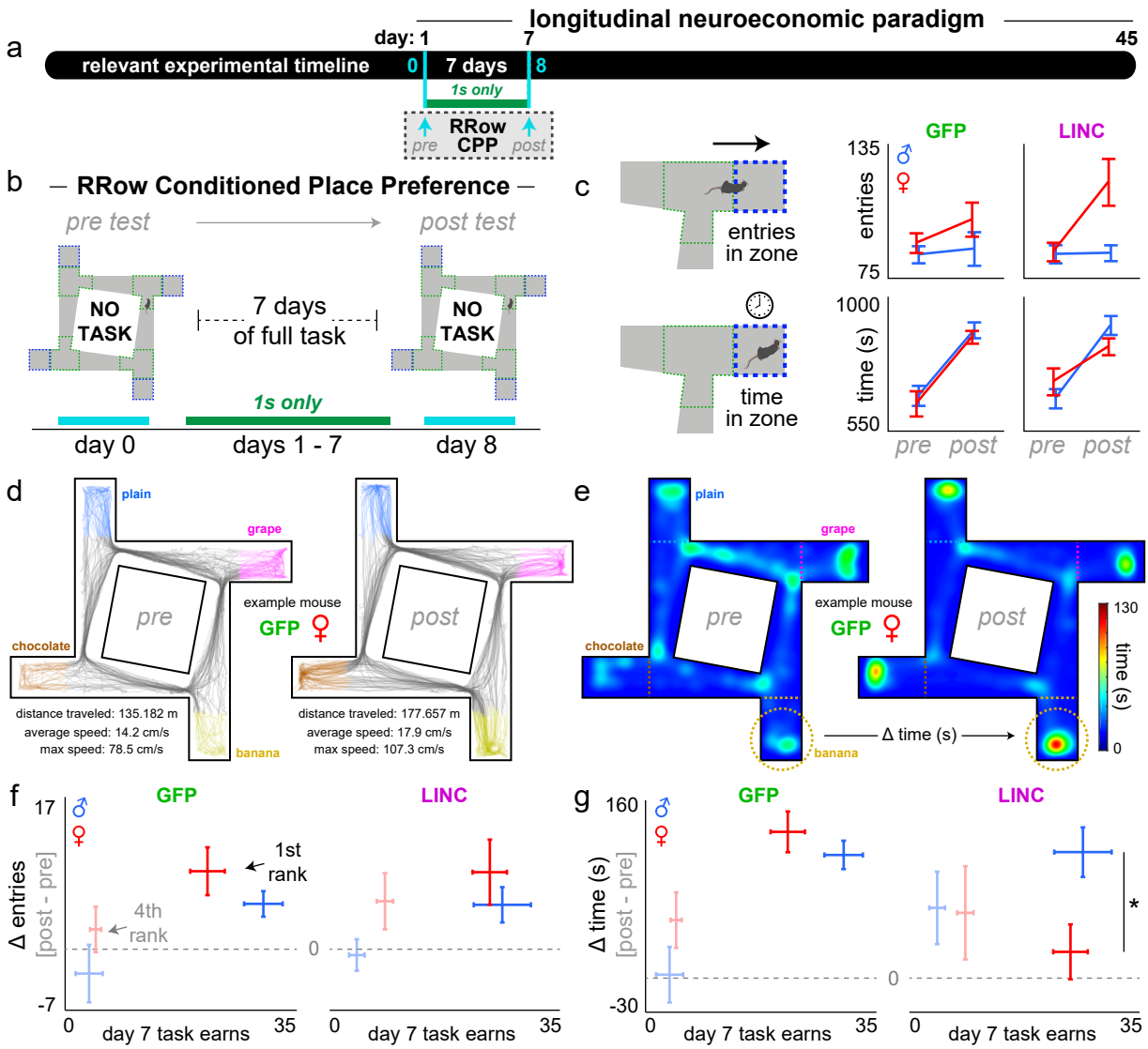
longitudinal neuroeconomic paradigm
a
day: 1
7
45
relevant experimental timeline
0
7 days
8
1s only
RRow CPP
pre
post
b
RRow Conditioned Place Preference
pre test
post test
NO TASK
7 days of full task
NO TASK
1s only
day 0
days 1 - 7
day 8
c
entries in zone
time in zone
GFP
LINC
entries
time (s)
135
75
1000
550
pre
post
d
plain
grape
chocolate
banana
pre
post
example mouse
GFP
distance traveled: 135.182 m
average speed: 14.2 cm/s
max speed: 78.5 cm/s
distance traveled: 177.657 m
average speed: 17.9 cm/s
max speed: 107.3 cm/s
e
Δ time (s)
130
0
time (s)
f
Δ entries [post - pre]
17
-7
1st rank
4th rank
day 7 task earns
0
35
g
Δ time (s) [post - pre]
160
-30
*

Figure 3

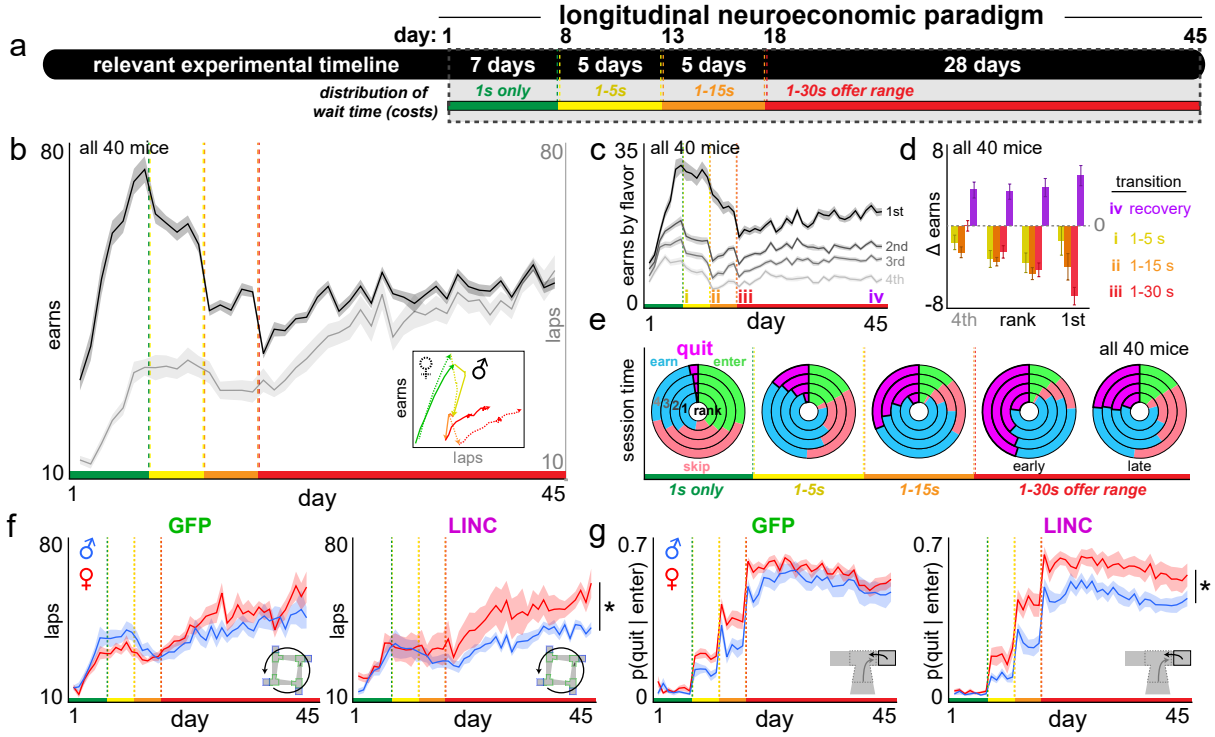
longitudinal neuroeconomic paradigm
a
day: 1
8
13
18
45
relevant experimental timeline
7 days
5 days
5 days
28 days
distribution of wait time (costs)
1s only
1-5s
1-15s
1-30s offer range
b
all 40 mice
earns
laps
day
c
all 40 mice
earns by flavor
1st
2nd
3rd
4th
i
ii
iii
iv
d
all 40 mice
Δ earns
transition
iv recovery
i 1-5 s
ii 1-15 s
iii 1-30 s
4th
rank
1st
e
quit
earn
enter
rank
skip
session time
all 40 mice
early
late
1s only
1-5s
1-15s
1-30s offer range
f
GFP
LINC
laps
day
g
GFP
LINC
p(quit | enter)
day

Figure 4

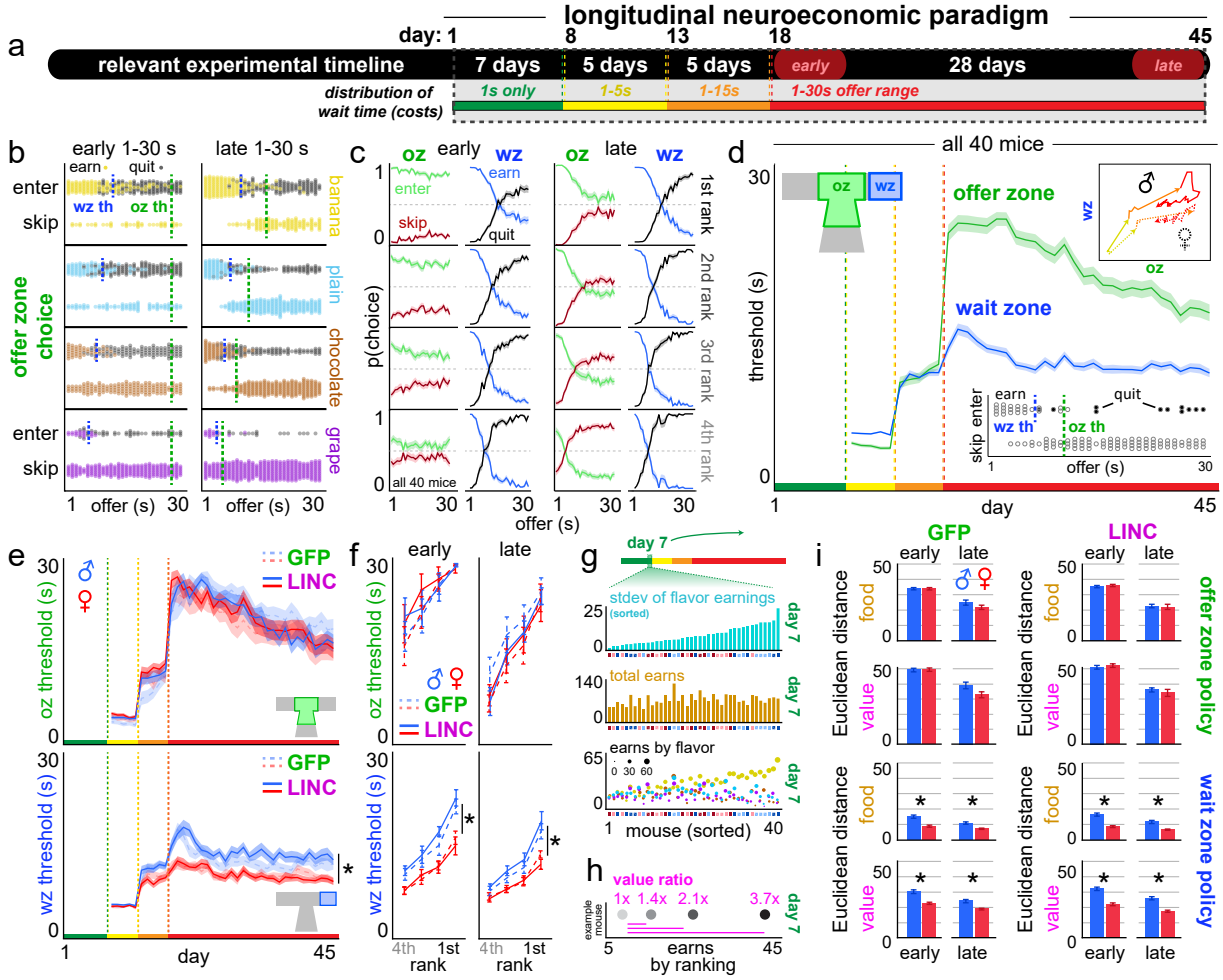
longitudinal neuroeconomic paradigm
a
day: 1
8
13
18
45
relevant experimental timeline
7 days
5 days
5 days
early
28 days
late
distribution of wait time (costs)
1s only
1-5s
1-15s
1-30s offer range
b
early 1-30 s
late 1-30 s
earn
quit
enter
skip
wz th
oz th
offer zone choice
banana
plain
chocolate
grape
offer (s)
c
oz
early
wz
late
enter
skip
earn
quit
all 40 mice
p(choice)
1st rank
2nd rank
3rd rank
4th rank
offer (s)
d
all 40 mice
oz
wz
offer zone
wait zone
threshold (s)
skip
enter
earn
quit
wz th
oz th
offer (s)
day
e
GFP
LINC
oz threshold (s)
wz threshold (s)
day
f
early
late
oz threshold (s)
wz threshold (s)
4th
1st
rank
g
day 7
stdev of flavor earnings
(sorted)
total earns
earns by flavor
mouse (sorted)
h
value ratio
1x
1.4x
2.1x
3.7x
example mouse
earns by ranking
i
GFP
LINC
early
late
Euclidean distance
food
value
offer zone policy
wait zone policy

Figure 5

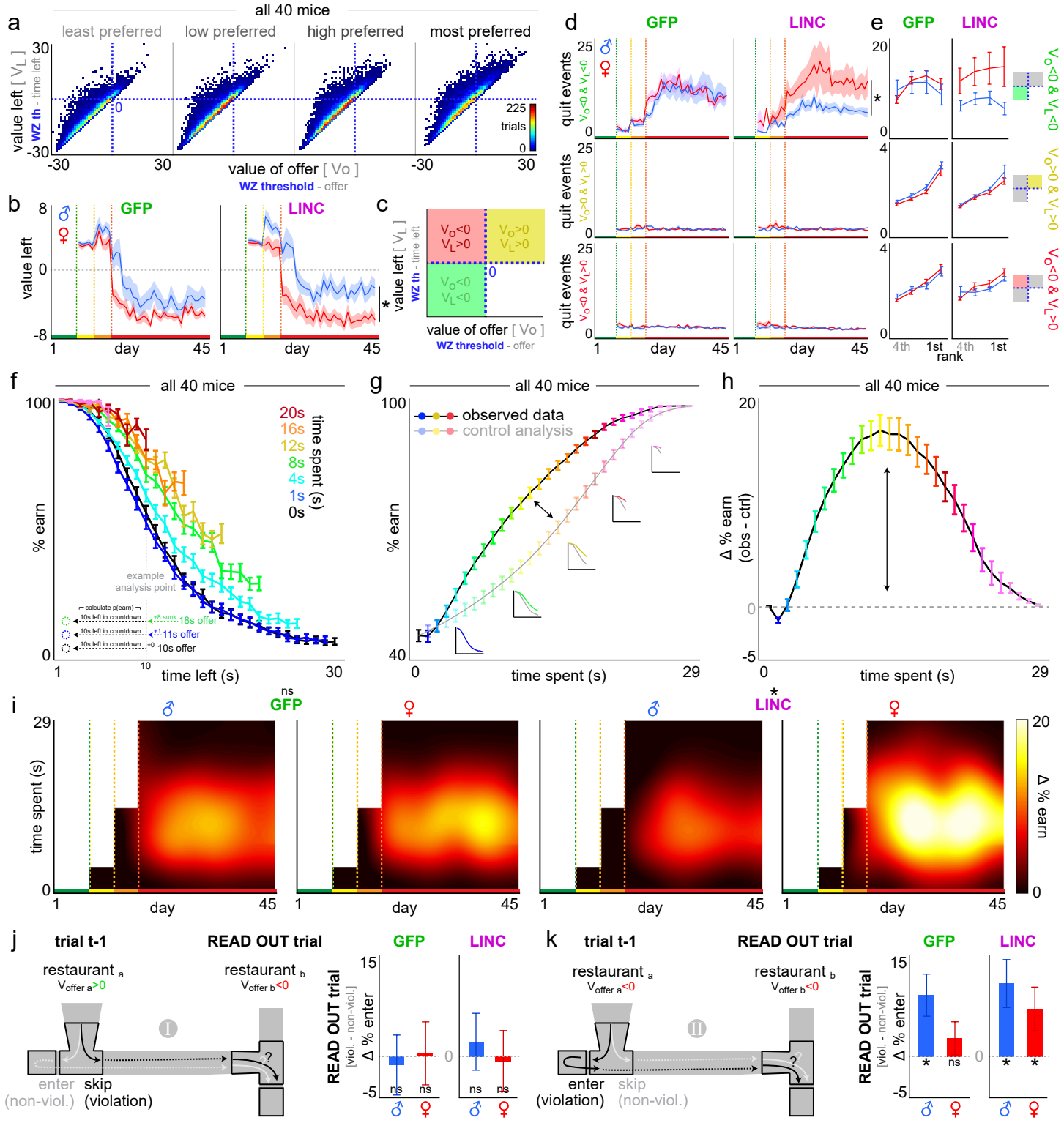
a
all 40 mice
least preferred
low preferred
high preferred
most preferred
value left [VL]
WZ th - time left
value of offer [Vo]
WZ threshold - offer
225
trials
b
GFP
LINC
value left
day
c
VO<0 VL>0
VO>0 VL>0
VO<0 VL<0
d
quit events
e
rank
4th
1st
f
time spent (s)
% earn
time left (s)
example analysis point
calculate p(earn)
10s left in countdown
18s offer
11s offer
10s offer
g
observed data
control analysis
h
Δ % earn (obs - ctrl)
i
time spent (s)
Δ % earn
j
trial t-1
READ OUT trial
restaurant a
restaurant b
enter (non-viol.)
skip (violation)
Δ % enter [viol. - non-viol.]
ns
k
enter (violation)
skip (non-viol.)

Figure 6

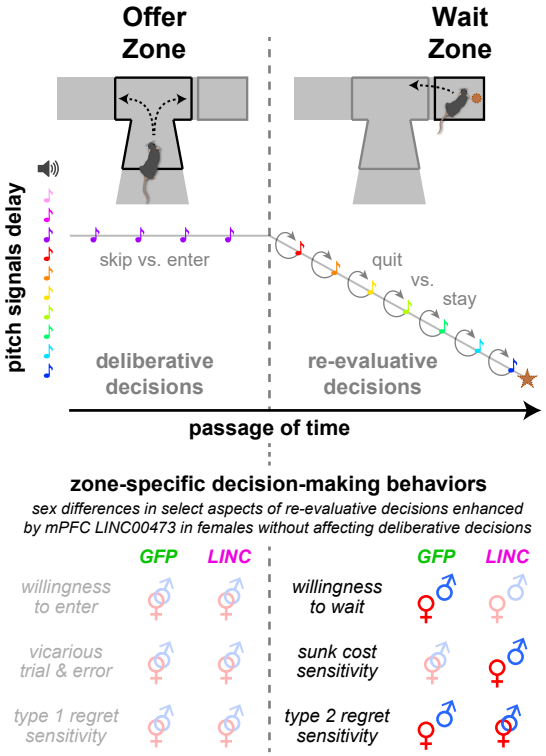
Offer Zone
Wait Zone
pitch signals delay
skip vs. enter
quit
vs.
stay
deliberative decisions
re-evaluative decisions
passage of time
zone-specific decision-making behaviors
sex differences in select aspects of re-evaluative decisions enhanced by mPFC LINC00473 in females without affecting deliberative decisions
GFP
LINC
willingness to enter
vicarious trial & error
type 1 regret sensitivity
GFP
LINC
willingness to wait
sunk cost sensitivity
type 2 regret sensitivity

Figure 7

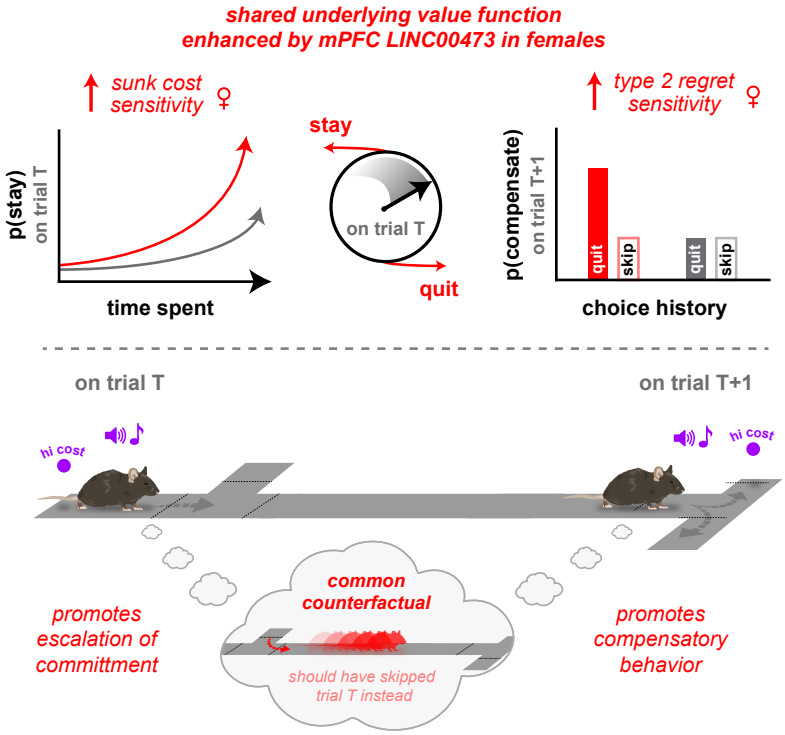
shared underlying value function
enhanced by mPFC LINC00473 in females
sunk cost sensitivity ♀
type 2 regret sensitivity ♀
p(stay)
on trial T
time spent
stay
on trial T
quit
p(compensate)
on trial T+1
quit
skip
quit
skip
choice history
on trial T
on trial T+1
hi cost
hi cost
common counterfactual
should have skipped trial T instead
promotes escalation of committment
promotes compensatory behavior

Supplementary Materials for

Change-of-mind neuroeconomic decision-making is modulated by LINC00473 in medial prefrontal cortex in a sex-dependent manner

Romain Durand-de Cuttoli[1], Orna Issler[2], Samantha M. B. Pedersen[4], Benjamin Yakubov[3], Nusrat Jahan[3], Aisha Abid[3], Susanna Kasparov[3], Kastalia Granizo[3], Sanjana Ahmed[3], Scott J. Russo[1], Eric J. Nestler[1,4], Brian M. Sweis*[1,4]

*Corresponding author. Email: brian.sweis@mountsinai.org

[1] Nash Family Department of Neuroscience, Friedman Brain Institute, Icahn School of Medicine at Mount Sinai, New York, NY 10029

[2] Neuroscience Institute, Department of Anesthesiology, Perioperative Care and Pain Medicine, and Department of Neuroscience and Physiology, NYU Langone, New York, NY 10016

[3] CUNY Hunter, New York, NY 10023

[4] Department of Psychiatry, Friedman Brain Institute, Icahn School of Medicine at Mount Sinai, New York, NY 10029

This PDF file includes:

Supplementary Text
Supplementary Figures 1-14

Supplementary Text

LINC00473 alters responses to limited task information during change-of-mind decisions.

We characterized how access to task-relevant sensory information may be critically important for sex- and LINC00473-dependent differences during change-of-mind decisions. This is important when considering what factors might be guiding on-going continuous re-evaluations and how much of this choice process depends on externally guided sensory information like that contained in the descending tone pitch cuing the countdown in the wait zone. After day 45, we tested mice for an additional 2 days during which tone playback on the task was silenced only in the wait zone but remained audible during offer zone presentations (**Supplementary Fig. 11a**). That is, mice had access to cost information signaled by tone pitch when making initial enter vs. skip decisions in the offer zone but received no countdown information once in the wait zone while making secondary re-evaluative decisions to quit or stay before earning rewards. This allows us to isolate properties of change-of-mind decision-making due to the internal mechanisms of re-evaluation in the absence of sensory information updated from the external world.

Overall, we found that males were more sensitive to this informational manipulation compared to females. Both GFP- and LINC00473-expressing males displayed a modest decreased number of laps run and total number of pellets earned, while female mice remained relatively unchanged between audible and silent conditions (laps [timepoint*sex]: F=10.678, p<0.01; laps [timepoint*virus]: F=0.449, p=0.507; earns [timepoint*sex]: F=10.124, p<0.01; earns [timepoint*virus]: F=0.002, p=0.969, **Supplementary Fig. 11b-c**). This task manipulation did not alter any overt changes in offer zone choices in any group as animals continued to discriminate the audible tones during cost-informed enter vs. skip decisions (offer: F=1186.818, p<0.0001; offer*timepoint: F=1.365, p=0.243; **Supplementary Fig. 11d**). Interestingly, when examining changes in wait zone thresholds, we found a significant sex difference when wait zone countdown information was withheld that was compounded by an additional LINC00473 effect in females only (**Supplementary Fig. 11e**). In males, compared to the audible condition, the lack of auditory information cuing mice on progress during the countdown in the silent wait zone condition drove an increase in wait zone thresholds for most preferred flavors (males: timepoint: F=22.976, p<0.0001; timepoint*virus: F=0.181, p=0.671 **Supplementary Fig. 11e**). Males also displayed a concomitant decrease in wait zone thresholds for least preferred flavors (males:

timepoint: F=19.561, p<0.0001; timepoint*virus: F=0.526, p=0.470, **Supplementary Fig. 11e**). These data indicate that, without cued auditory guidance in the wait zone, males were more patient waiting for favorite flavors and less patient waiting for least favorite flavors (defined by a change in the indifference point of earn outcomes as a function of the trial's starting offer). Conversely, GFP-expressing females only displayed a decrease in wait zone thresholds for less preferred flavors, with no change in thresholds for most preferred flavors (**Supplementary Fig. 11e**). LINC00473-expressing females however did not display any changes in wait zone thresholds in any restaurant compared between audible and silent wait zone conditions (females: timepoint [most preferred]: F=2.569, p=0.112; timepoint*virus [most preferred]: F=0.137, p=0.712; timepoint [least preferred]: F=12.185, p<0.0001; timepoint*virus [least preferred]: F=8.901, p<0.01).

These data indicate LINC00473-expressing females valued offers in a consistent manner with or without externally guided information, suggesting that their internal measures of time or how they hold and maintain information from the offer zone in working memory may be more stable. Strikingly, this effect of LINC00473 was specific to when information was manipulated only in the wait zone, and did not appear if information was manipulated in just the wait zone nor in both the offer zone and the wait zone (**Supplementary Fig. 12-13**).

When examining quit times in the wait zone, all mice displayed a modest increased latency to make quit decisions in the silent condition compared to the audible condition (timepoint: F=11.764, p<0.001; sex: F=2.358, p=0.126; virus: F=0.836, p=0.361, **Supplementary Fig. 11f**). Finally, when examining sensitivity of change-of-mind quitting behavior to the passage of time already spent waiting in the wait zone, we found that the silent condition unmasked a sex difference in GFP-treated mice whereby females show increased sensitivity to time expenditures compared to males – a sex difference that was previously only apparent during the audible condition in LINC00473-expressing groups (time spent: F=97.196, p<0.001; sex: F=36.989, p<0.0001; virus: F=1.899, p=0.168; **Supplementary Fig. 11g**). These data highlight how the integration between external cues and internally generated value representations is unique during change-of-mind decisions and is differentially processed in LINC00473-treated females. This implies that mPFC function is critical for different ways in which individuals may rehearse or update information during ongoing re-evaluations with vs. without explicit sensory cues, specifically during change-of-mind decisions.

Supplementary Figures 1-14

Supplementary Figure 1

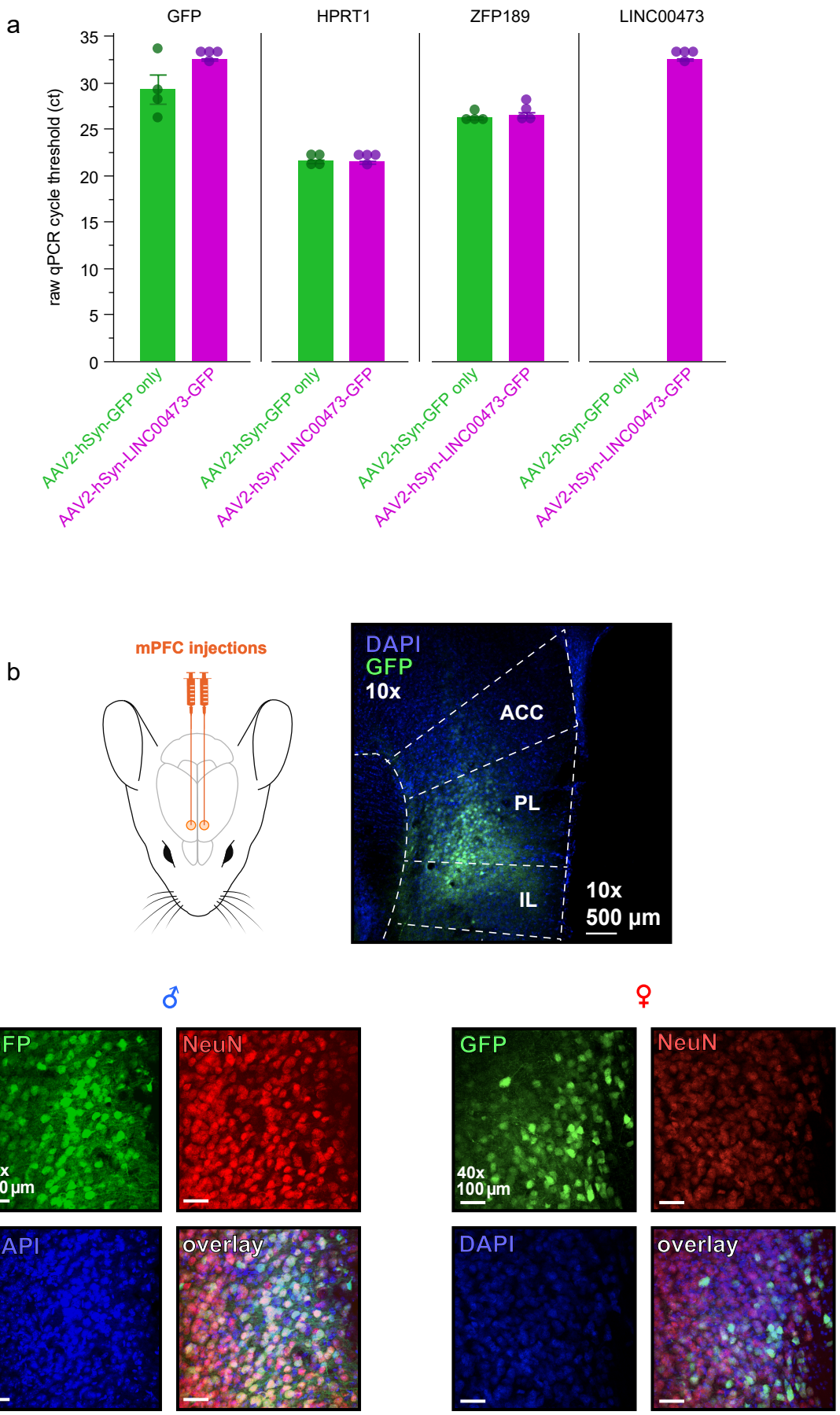

Supplementary Fig. 1 | Validation of newly packaged adeno-associated virus expression of LINC00473. a Raw qPCR cycle threshold count (ct) obtain from mPFC tissue punches extracted from mice separately transfected with either AAV2-hSyn-GFP (control) or AAV2-hSyn-LINC00473-GFP (treatment). qPCR readouts obtained for expression levels of GFP, HPRT1 (housekeeping), ZFP189 (another known regulator of stress-resilience), and LINC00473. Note similar levels of expression of GFP (t=2.03, p=0.089), HPRT1 (t=0.41, p=0.693), and ZFP189 (t=0.91, p=0.396) between control and treatment viruses. Also note no detectable levels of LINC00473 in mice transfected with the control virus, as this is not endogenously expressed in mice. Dots represent individual samples. Error bars represent ±1 SEM. **b** Representative images of surgical targeting of mPFC bilaterally. 10x magnification image shows representative virus transfection of GFP toward ventral mPFC (generally including both prelimbic and infralimbic subregions). 40x images show representative targeting in both male and female mice depicting virus transfection of GFP, NeuN staining of neurons, and DAPI of cell bodies, both in separate channels and overlaid.

Supplementary Figure 2

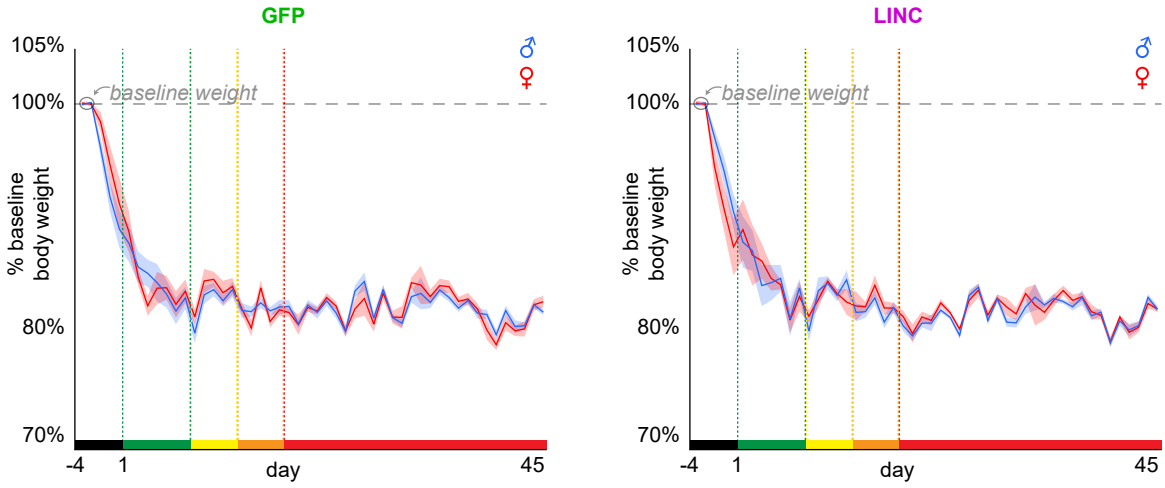

Supplementary Fig. 2 | Bodyweight measurements. Percentage of a 2-day average (circled in gray, horizontal dashed line for reference) of baseline body weight obtained 4 days prior (black epoch) to the start of the longitudinal Restaurant Row paradigm. During this period (black epoch), mice were food restricted and fed a limited ration to intentionally decrease weights to approximately 80-85% of baseline that was steadily maintained throughout the remainder of the experiment (days 1-45, see main Fig. 1 for an explanation of the color-coded epochs of testing across the paradigm). These body weights reflect the measurements immediately before task performance on each day of testing. There were no differences in percentage baseline bodyweight between groups (virus: F=0.292, p=0.593; sex: F=0.118, p=0.733). Shaded area represents ±1 SEM.

Supplementary Figure 3

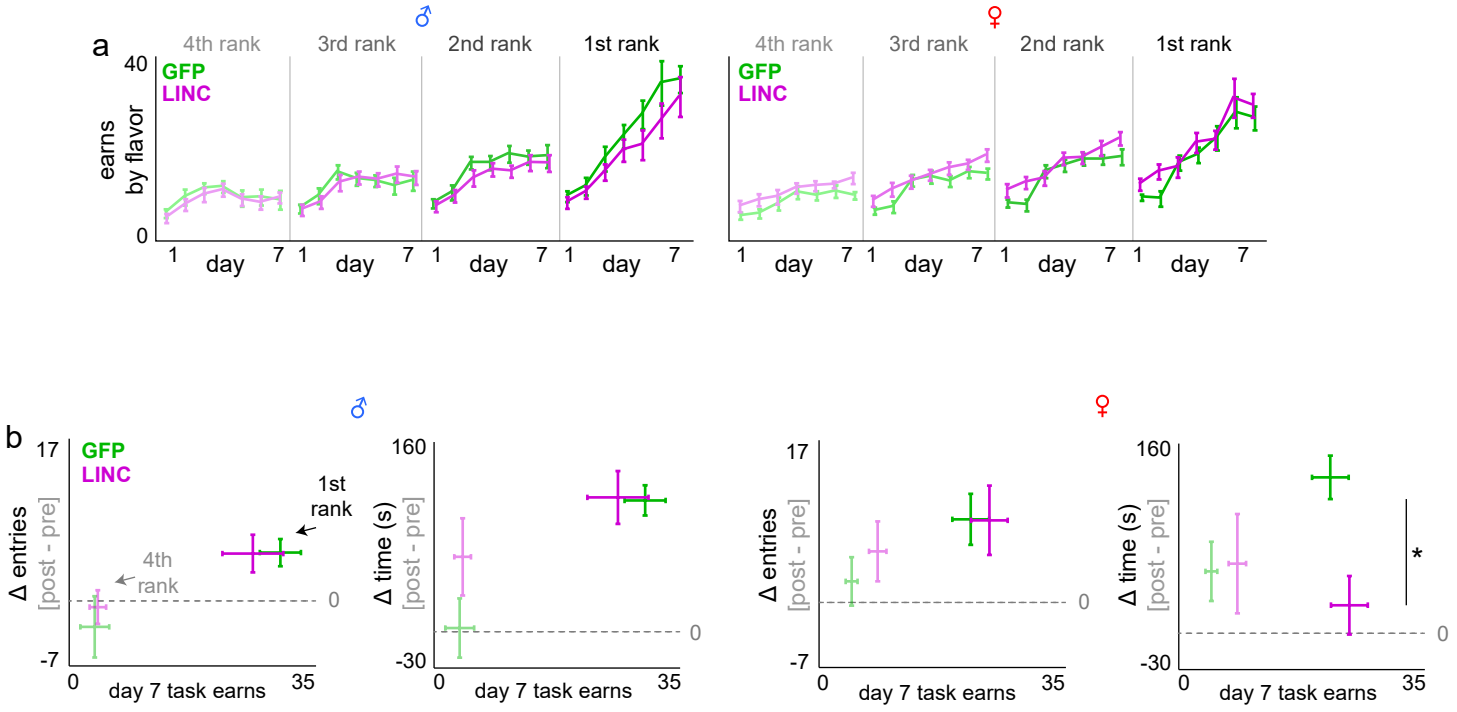

Supplementary Fig. 3 | Redisplay of earns by flavor and CPP probe sessions. Figures redisplayed separating sex and superimposing GFP vs. LINC00473 groups. **a** Redisplay from main Fig. 1. Average number of rewards earned across the first week of testing split by flavors ranked from least to most preferred based on each day's end-of-session totals. **b** Redisplay from main Fig. 2. Delta scores of total number of entries into and total time spent at each reward site subtracting post (day 8) minus pre (day 0) sessions. Two restaurants' reward sites depicted: most and least preferred restaurants. Error bars represent ±1 SEM.

Supplementary Figure 4

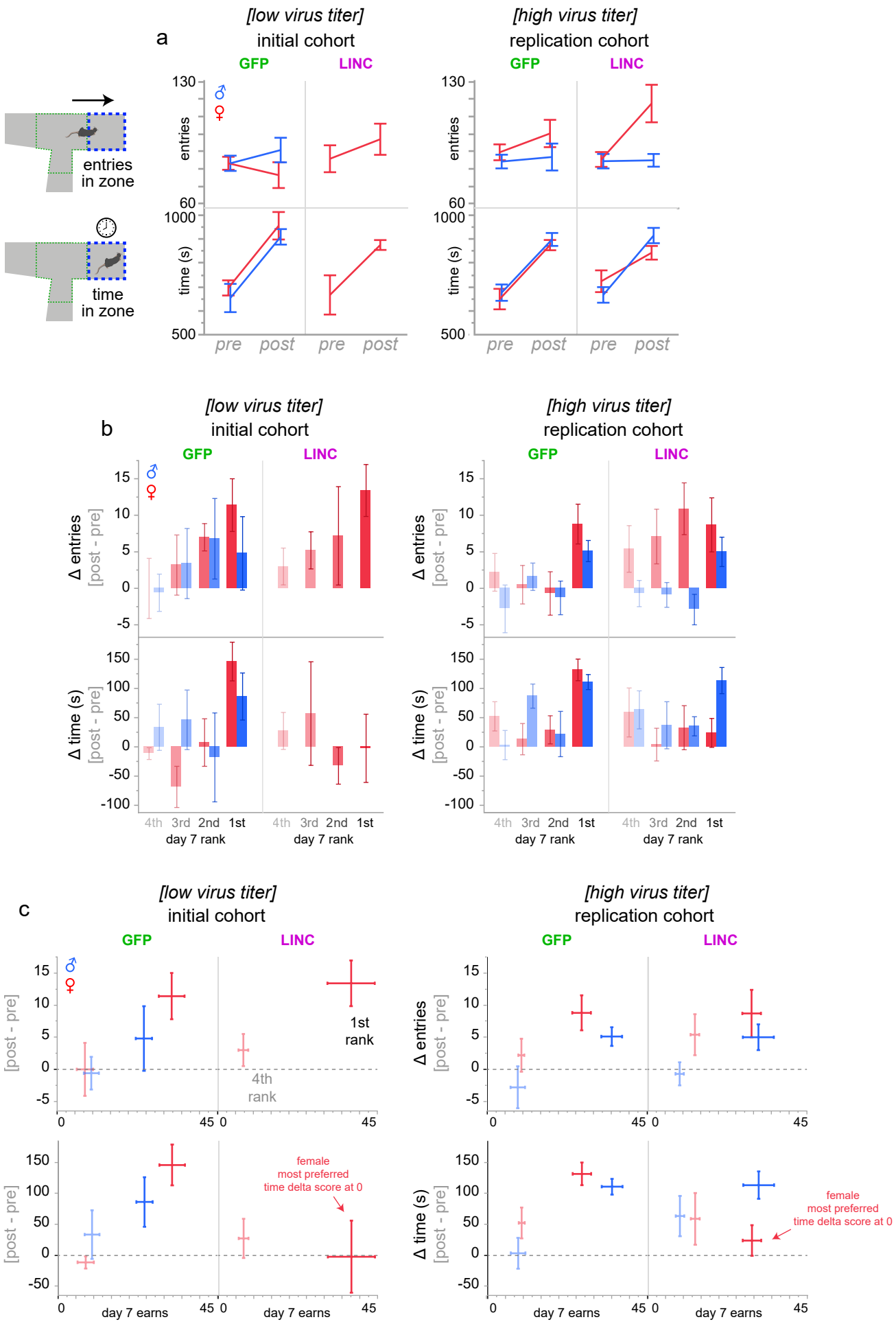

Supplementary Fig. 4 | Replication cohort of two different virus titers on sex-specific Restaurant Row conditioned place preference (CPP) findings. Animals were placed in the arena free to roam for 20 min on day 0 and day 8 of the experimental timeline but with no active task to obtain pre-task baseline and post-task experience-related exploratory behavior (see main Fig. 2). **a** Total number of entries and total time spent in the wait zone, aggregated in all restaurants. Depicting findings from independent cohorts: surgeries and behavioral experiments were carried out across separate calendar months and using different virus titers. **b** Delta scores in change of entries and time comparing post (day 8) minus pre (day 0) time points split by restaurants ranked according to rewards earned on the active task on day 7. **c** Data from (b, only 1st and 4th ranking restaurants) replotted with number of rewards earned on day 7 on the x-axis. Horizontal dashed gray line indicates delta score of 0. LINC00473 expression in mPFC abolished CPP behavior in most preferred restaurants only in females and only in the time but not entry domain, replicated in both cohorts. +Sign-test on delta score of time: low virus cohort: male GFP: (t=2.142, p<0.05); female GFP: (t=4.424, p<0.01); female LNC: (t=0.04, p=0.516); high virus cohort: male GFP: (t=8.681, p<0.0001); male LINC: (t=5.087, p<0.001); female GFP: (t=7.157, p<0.0001); female LNC: (t=0.962, p=0.181). +Sign-test on delta score of entries: low virus cohort: male GFP: (t=0.955, p=0.197); female GFP: (t=3.155, p<0.05); female LNC: (t=3.766, p<0.01); high virus cohort: male GFP: (t=3.520, p<0.01); male LINC: (t=2.493, p<0.05); female GFP: (t=3.236, p<0.01); female LNC: (t=2.355, p<0.05). Error bars represent ±1 SEM.

Supplementary Figure 5

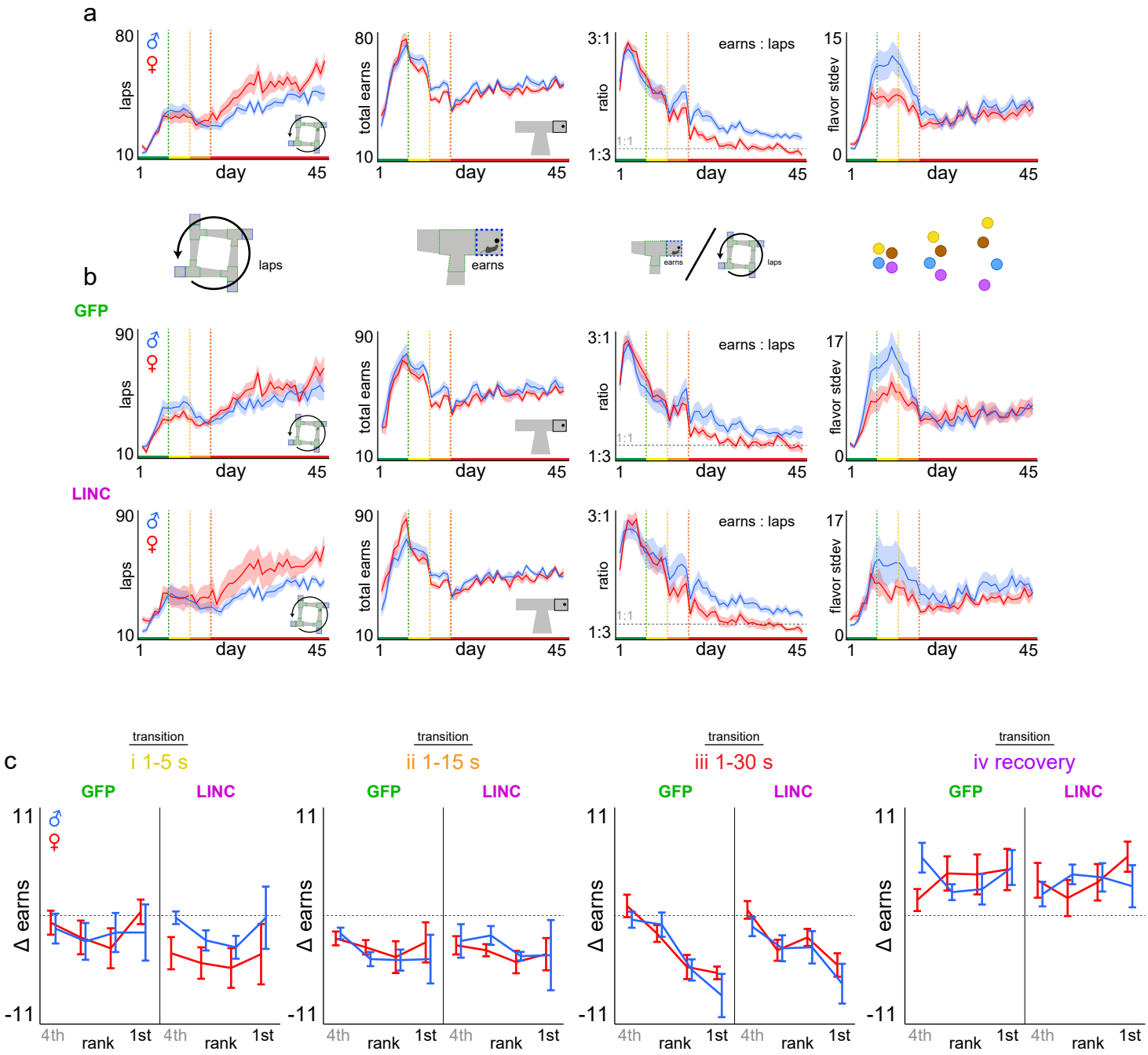

Supplementary Fig. 5 | Basic Restaurant Row laps and earnings metrics across testing. a Overall sex difference comparisons between males and females (collapsing across GFP and LINC00473 virus treatment within each sex). Average number of laps run in the correct direction (sex*day: F=78.040, p<0.0001), total rewards earned (sex*day: F=1.331, p=0.249), ratio of earns / laps (sex*day: F=28.155, p<0.0001), and standard deviation of earns among flavors (sex*day: F=13.014, p<0.001). **b** Data from (a) split by GFP and LINC groups: laps (sex*virus*day: F=0.008, p=0.927), total earns (sex*virus*day: F=7.470, p<0.01), ratio of earns / laps (sex*virus*day: F=1.130, p=0.288), standard deviation of earns by flavor (sex*virus*day: F=15.486, p<0.0001). Statistical tests from (a) and (b) were performed on the entire experimental timeline (days 1-45). **c** Data from main Fig. 3d split by sex and virus groups depicting change in rewards earned in each restaurant comparing two days at each color-coded transition point. Delta scores calculated by subtracting the following: i, day 8-7 (yellow, rank: F=1.361, p=0.259; sex*virus: F=0.017, p=0.897); ii, day 13-12 (orange, rank: F=1.123, p=0.343; sex*virus: F=0.086, p=0.769); iii, day 18-17 (red, rank: F=18.116, p<0.0001; sex*virus: F=0.076, p=0.783); iv, day 45-18 (purple, rank: F=0.603, p=0.614; sex*virus: F=0.375, p=0.542). Shaded area and error bars represent ±1 SEM.

Supplementary Figure 6

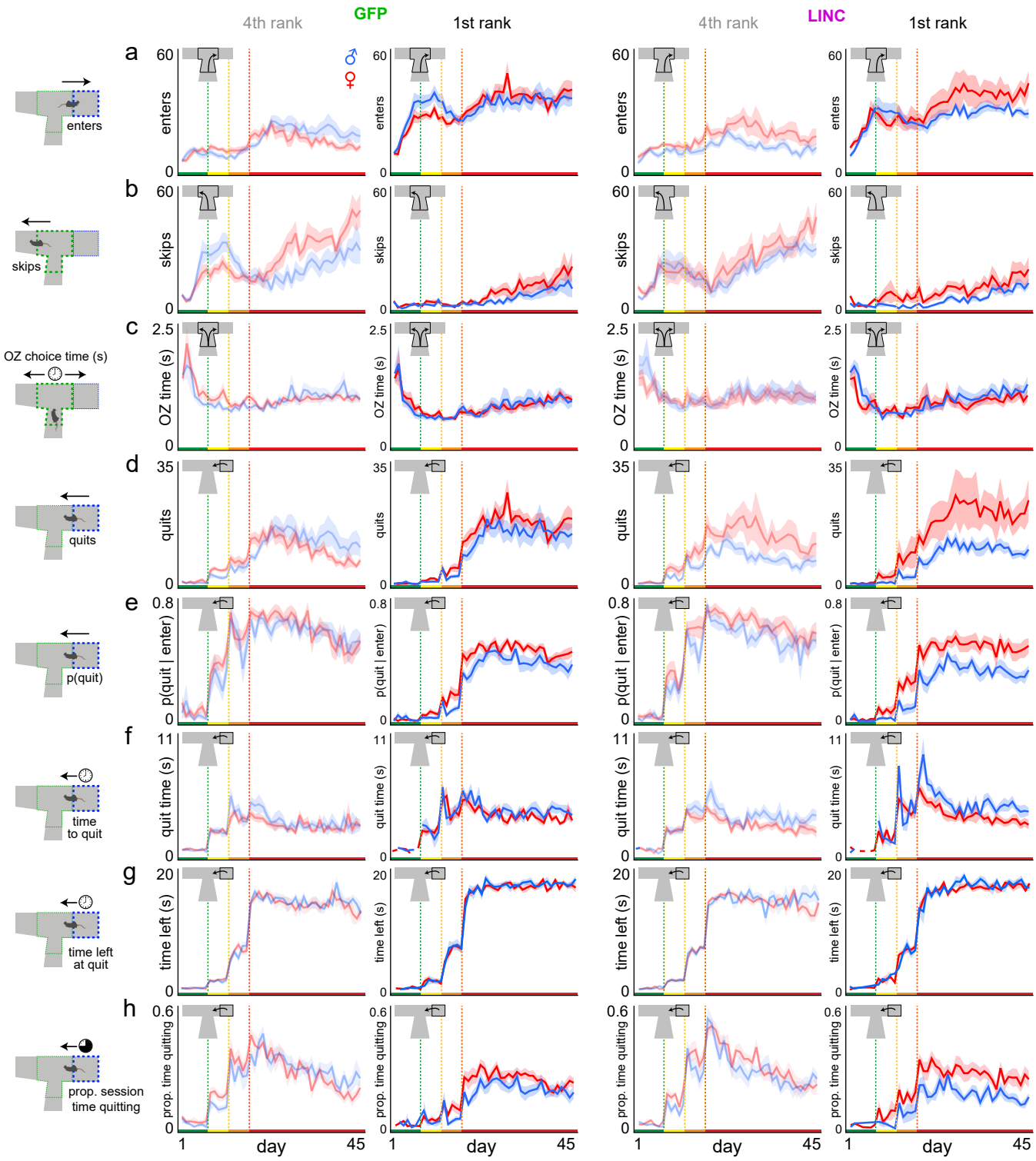

Supplementary Fig. 6 | Restaurant Row choice metrics split by flavor ranking across testing. a Average number of enter decisions made in the offer zone split by sex and virus treatment groups as well as the 4th and 1st ranking restaurant (sex*rank*day: F=16.043, p<0.0001; sex*virus*rank*day: F=3.967, p<0.01). **b** Number of skip decisions made in the offer zone (sex*rank*day: F=9.894, p<0.0001; sex*virus*rank*day: F=2.617, p<0.05). **c** Offer zone reaction time before making an enter or skip decision calculated from offer zone entry (tone onset) to either a right turn into the wait zone (enter) or a left turn into the hallway (skip) (sex*rank*day: F=0.325, p=0.808; sex*virus*rank*day: F=2.186, p=0.087). **d** Number of quit decisions made in the wait zone during a countdown (sex*rank*day: F=11.725, p<0.0001; sex*virus*rank*day: F=1.216, p=0.302). **e** The probability of quitting in the wait zone given the animal entered (sex*rank*day: F=4.145, p<0.01; sex*virus*rank*day: F=0.463, p=0.708). This normalizes the likelihood of quitting to enter frequency. **f** Wait zone latency to quit reaction time from countdown onset (wait zone entry) until mice leave the wait zone prematurely (sex*rank*day: F=1.427, p=0.233; sex*virus*rank*day: F=3.160, p<0.05). **g** The amount of time left remaining in the countdown required to finish earning a reward at the moment of quitting in the wait zone. **h** Proportion of session time within each restaurant spent engaged in quitting behavior in the wait zone. Statistical tests here were performed on the entire experimental timeline (days 1-45). Shaded area represents ±1 SEM.

Supplementary Figure 7

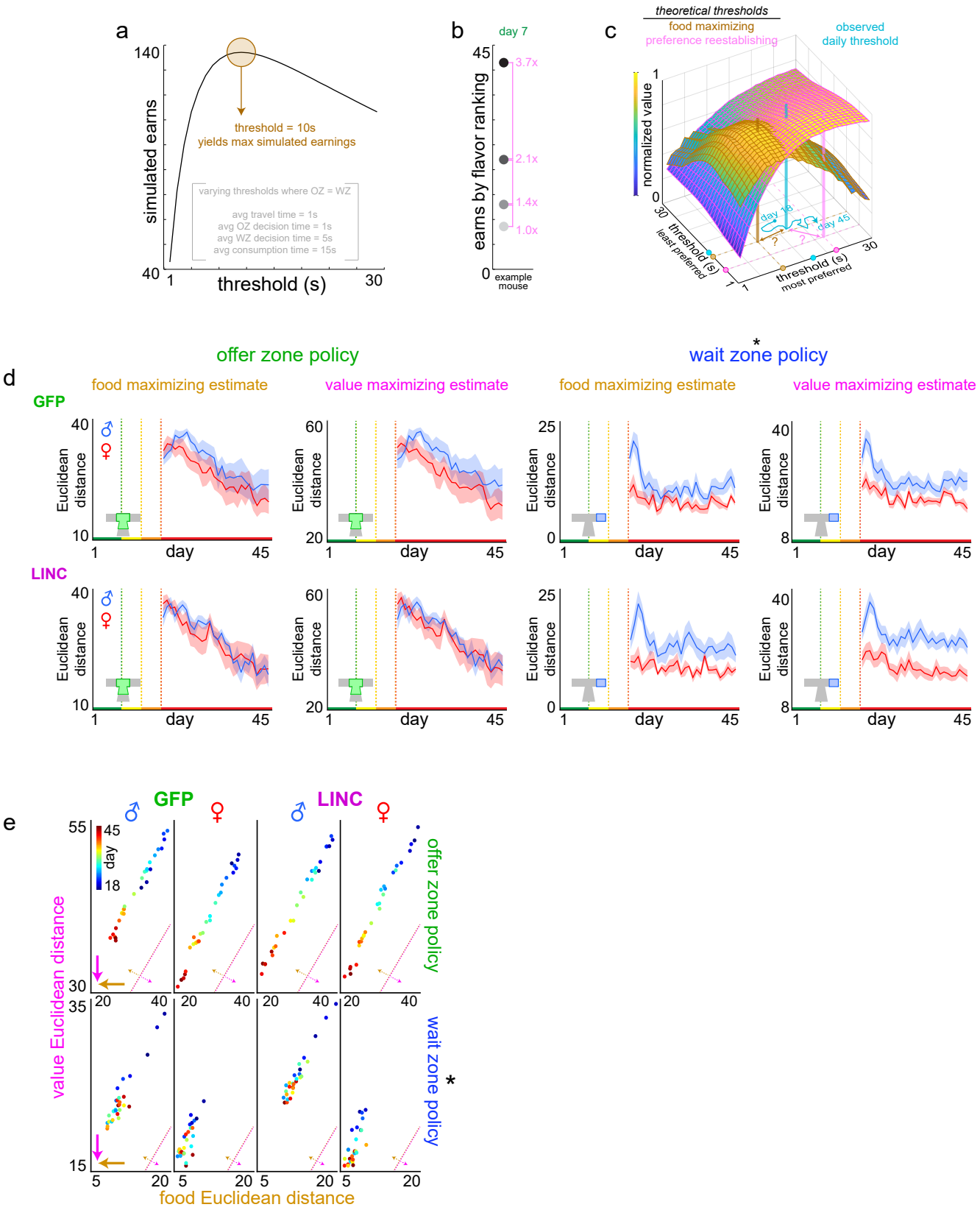

Supplementary Fig. 7 | Longitudinal economic analysis of decision policy optimization for food security vs. subjective value. Analysis underlying data from main Fig. 4g-i derived from Durand-de Cuttoli et al 2023 *Biological Psychiatry* [43]. See **Methods** for more details on this analysis. **a** Computer Restaurant Row simulation of total number of pellets earned. The ideal threshold required to obtain the theoretical maximum number of pellets when ignoring flavor preferences was empirically determined to be 10 s. **b** Relative ratio of earns among restaurants for an example mouse on day 7 between the flavor rankings (i.e., this mouse had a 3.7 : 2.1 : 1.4 : 1 ratio of earns across flavors capturing a summary of idealized relative subjective value for this mouse when all offers were 1 s only). **c** Two intersecting planes of decision policies that yield varying amounts of theoretical value either for maximal food intake (as determined by computer simulations, brown plane) or subjective value (as determined by multiplying simulation output of flavor earnings by day 7's preference ratios on a mouse-by-mouse basis, pink plane) when in a reward-scarce environment (1 to 30 s offers). Here, only two decision policy dimensions (least preferred and most preferred restaurants) of the four dimensions (all four ranked restaurants) are displayed. Both planes are normalized to each's min and max values for the purpose of plotting both in the same space while preserving the threshold coordinate locations that achieve either theoretical maximum (brown [location always fixed at threshold coordinates of 10 s] or pink beacons [location of discovered threshold coordinates that vary from mouse-to-mouse]). Actual observed daily decision policies represented by the cyan beacon wander throughout this space from day 18 to 45 in a reward-scarce environment. Trajectories projected to the floor of this display trace out individual mouse decision policy paths. Example coordinates of brown, pink, and cyan beacons illustrated as dots on the x and y axes. Euclidean distance from cyan coordinates to either brown or pink coordinates were calculated (question mark symbols). **d** Euclidean distances from observed decision policies in the offer zone (left) or wait zone (right) to either food (brown) or preference (magenta) theoretical maximum across testing in a reward-scarce environment split by GFP (top) and LINC (bottom) groups and sex. Offer zone: food distance: day: F=49.362, p<0.0001; sex: F=1.115, p=0.298; virus: F=0.008, p=0.929; value distance: day: F=42.042, p<0.0001, sex: F=1.546, p=0.221; virus: F=0.001, p=0.989; Wait zone: food distance: day: F=16.774, p<0.001, sex: F=13.796, p<0.001; virus: F=0.598, p=0.445; value distance: day: F=38.046, p<0.0001, sex: F=18.034, p<0.0001; virus: F=0.261, p=0.613. **e** Data from (d) redisplayed showing the Euclidean distance between observed decision policies each day from days 18-45 (cool to warm colors, each dot indicates group average per day) to theoretical policies that could achieve either maximal food (x-axis) or maximal subjective value (y-axis) for offer zone and wait zone thresholds. Inset diagonal lines indicate reference point for the 1:1 unity line. Bold brown and magenta arrows pointing toward the origin represent direction of reduced Euclidean distance vectors that optimize either food or value, respectively. Dashed brown and magenta arrows pointing off diagonal from the unity line represent if the decision policy is biased to prefer food vs. value. Prominent sex difference, without apparent effect of LINC00473 expression in mPFC, in present in wait zone but not offer zone economic decision policies. Shaded area represents ±1 SEM.

Supplementary Figure 8

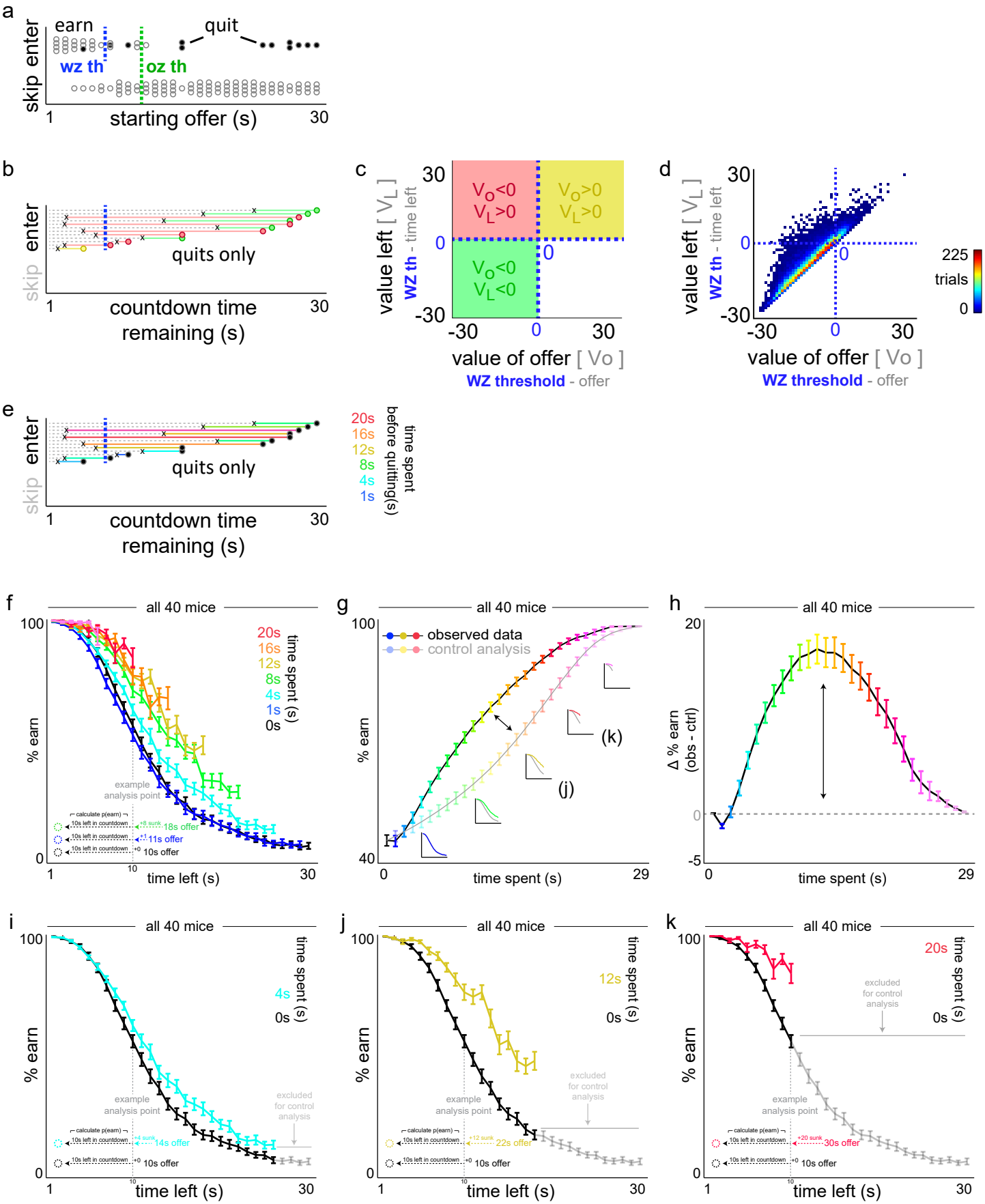

Supplementary Fig. 8 | Visual explanation of characterizing quitting behavior. a Example choice data from a single mouse, single session, in a single restaurant. Individual dots represent individual trials. Offer zone outcomes plotted on the Y-axis as a function of the cued offer at the start of each trial along the X-axis. Of the enter trials, wait zone outcomes represent earns as open circles and quits as closed circles. Vertical dashed green and blue lines indicate the offer zone and wait zone thresholds, respectively. Note: the only temporal data shown here is the starting delay at the onset of the trial, and how each trial terminates as either a skip, enter then earn, or enter then quit. Only panels b-e include temporal data about how long it took animals to quit, for instance, and conversely, how much time was remaining in the countdown at the moment of quitting. **b** Data from (a) showing only the quit trials. Horizontal solid-colored lines extending from each dot leftward represent how much time was spent waiting before the mouse decided to quit. The point at which the mouse quit is represented by the black "x" symbol. The remaining dashed gray lines extending from the "x" leftward thus represent the amount of time remaining in the countdown at the moment of quitting. The relationship between one's own wait zone threshold (vertical dashed blue line) and whether or not (i) the starting offer [circle] is to the right or the left of the wait zone threshold and (ii) the amount of time remaining at the moment of quitting ["x"] is to the right or the left of the wait zone threshold determines which quadrant each quit event belongs to in panels (c-d). Thus, each quit event is color coded based on its placement in the quadrants in (c-d). **c-d** Offer value plotted against value left can divide up this quit space into a two-by-two matrix based on the sign of each value term [i.e., if the starting offer was above or below one's own wait zone threshold [represented by the dashed blue 0 lines] and if the time left at the moment of quitting was above or below one's own wait zone threshold]. Data can only possibly exist in the three colored green, yellow, and red quadrants. Schematic in (c) and actual example data from main Fig. 5a re-displayed here. **e** Lastly, the time spent waiting before quitting is color-coded in yet another way, here based on how much time was already invested prior to the quit decision being made. Thus, this can separate rapid quit events from longer latencies to quit. These measures form one dimension of the data used in the sunk cost analysis, which also factors in varying amounts of time left remaining (horizontal gray dashed lines that represent the residual time at the moment of quitting). **f-k** Explanation of sunk cost and control analysis. (f-h) Redisplay of data from main Fig. 5f-h. Sunk cost analysis of staying behavior in the wait zone, demonstrated using all mice. (f) The likelihood of staying in the wait zone and earning a reward (e.g., not quit) is plotted as a function of time left in the countdown along the x-axis and time already spent waiting orthogonally in color. Note the black 0 s time spent curve represents animals having just entered the wait zone from the offer zone. Inset vertical dashed gray line illustrates an example analysis point comparing three sunk cost conditions originating from different starting offers but matched at 10 s left. Data from (f) dimensioned reduced in (g) collapsing across time left, instead highlighting the grand mean of each time spent sunk cost condition (color and x-axis). Insets depict data from curves in (f) are collapsed into the observed (sunk condition) and control (0 s condition) lines. Difference between curves in (g) are plotted in (h) in order to summarize the envelope of the overall effect of time already spent on escalating the commitment of staying in the wait zone. Horizontal dashed line represents a delta score of 0. (i-k) Redisplay of data from (f) but for three sunk cost conditions indicated in the insets in (g, 4 s cyan in i, 12 s gold in j, 20 s red in k) with the 0 sunk cost condition (black curve) repeated in each panel. Because each colored sunk cost curve derives from trials where the starting offer cost is higher than the matched time left value of the 0 s cost condition, some data points do not exist and are missing from the sunk cost curve on the rightward end. Thus, when reducing dimensions, to control for the inflated summary calculations of % earn due to missing data alone, the control analysis iteratively excludes matched data from the black 0 s sunk curve (highlighted in gray) before collapsing data to yield the resultant control curve in (g). Error bars represent ±1 SEM.

Supplementary Figure 9

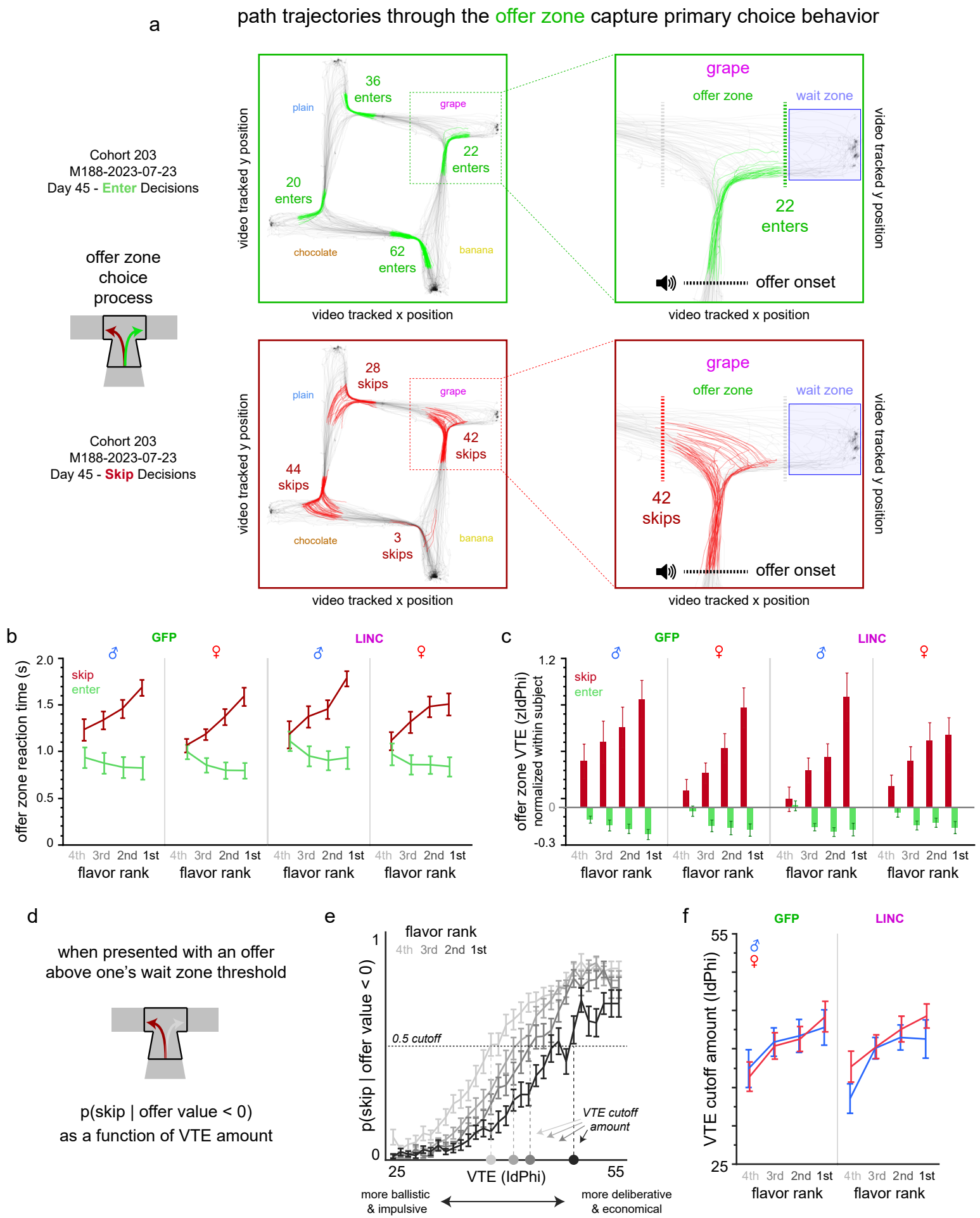

Supplementary Fig. 9 | Video-tracking analysis of choice behavior in the offer zone. a Example video tracking data during a full 30-min session obtained from one example mouse (M188) taken from day 45 of testing. Track plots display X-Y body centroid position data of the mouse at 30 fps as the animal navigates the maze arena performing the task. All path trajectories through the offer zone on each trial beginning at trial onset (triggered by body centroid position crossing the stem of the entrance into the restaurant, which also triggers the auditory cue onset) until animals turn right and enter the wait zone (triggered by body centroid position crossing the wait zone boundary, which then triggers the countdown onset) are color-coded in green. All other position data are color-coded in gray. The number of enter decisions made in each restaurant are displayed. Zoomed-in example shows a closer depiction of the grape restaurant. The same data is redisplayed again but for skip decisions color-coded in red. Note the significantly greater heterogeneity in path trajectories through the offer zone, including a greater mix of heading-direction reorientation events before ultimately registering a skip outcome (triggered by body centroid position crossing the left boundary of the offer zone as animals enter the hallway connecting to the next restaurant) compared to enter decisions that are more uniformly ballistic and without path reorientations. **b** Offer zone reaction time measures plotted as a function of restaurant flavor preferences ranked from least to most preferred and split by whether or not mice made a skip or enter decision. Latencies to skip or enter were measured from trial and cued offer onset (traversing the stem entrance of each restaurant) until body centroid position crosses the rightward wait zone entry point or leftward hallway entry point. Significant interaction between choice outcome (enter vs. skip) and flavor ranking (F=14.201, p<0.0001) but no significant effects of sex (F=1.170, p=0.280) or virus (F=0.253, p=0.615). Reaction time alone does not necessarily capture individual differences in how ballistic vs. tortuous path trajectories can be through the choice point. Vicarious trial and error (VTE) behavior has been previously shown to capture heading-direction reorientation events and correlates with neural representations of deliberative decision-making processes (high VTE events) vs. the lack thereof (low VTE events). The physical “hemming and hawing” characteristic of VTE is best measured by calculating changes in velocity vectors of discrete body X and Y positions over time as dx and dy. From this, we can calculate the momentary change in angle, *Phi*, as *dPhi*. When this metric is integrated over the duration of the pass through the offer zone, VTE is measured as the absolute integrated angular velocity, or *IdPhi*, until either a skip or enter decision was made. This measure importantly is normalized within subject by z-scoring *IdPhi* values across all choices within a given session on a mouse-by-mouse basis, and then subsequently splitting the data by choice outcome and restaurant in order to appreciate within subject differences of how different types of choices and in different restaurants elicit varying amounts of either high or low VTE events. Significant interaction between choice outcome (enter vs. skip) and flavor ranking (F=19.819, p<0.0001) but no significant effects of sex (F=0.181, p=0.671) or virus (F=0.374, p=0.541). **d-f** Analysis of VTE behavior depicting the probability of skipping in the offer zone a negatively valued offer (offer above one’s wait zone threshold) as a function of binned VTE amounts. (e) Skipping probability given offer value <0 as a function of VTE amount split by restaurants ranked by flavor preferences for all 40 mice. Horizontal dashed line indicates a probability cutoff of 0.5 used to determine the X-intercept (vertical dashed lines shaded per restaurant), or amount of VTE displayed in order to reliably skip an economically disadvantageous offer. (f) VTE cutoff amount split by flavor rank, sex, and LINC00473 treatment. Significant effect of flavor ranking (F=9.372, p<0.0001) but no significant effects of sex (F=0.464, p=0.497) or virus (F=1.330, p=0.251). Data in (b-f) collapsed across the 1-30 s epoch (days 18-45). These data indicate that LINC00473 treatment nor sex has an impact on offer zone choice processes, including leaving intact deliberative behaviors that interact with the type of decision being made and counteract pre-potent impulsive responses to enter depending on the degree of flavor preference.

Supplementary Figure 10

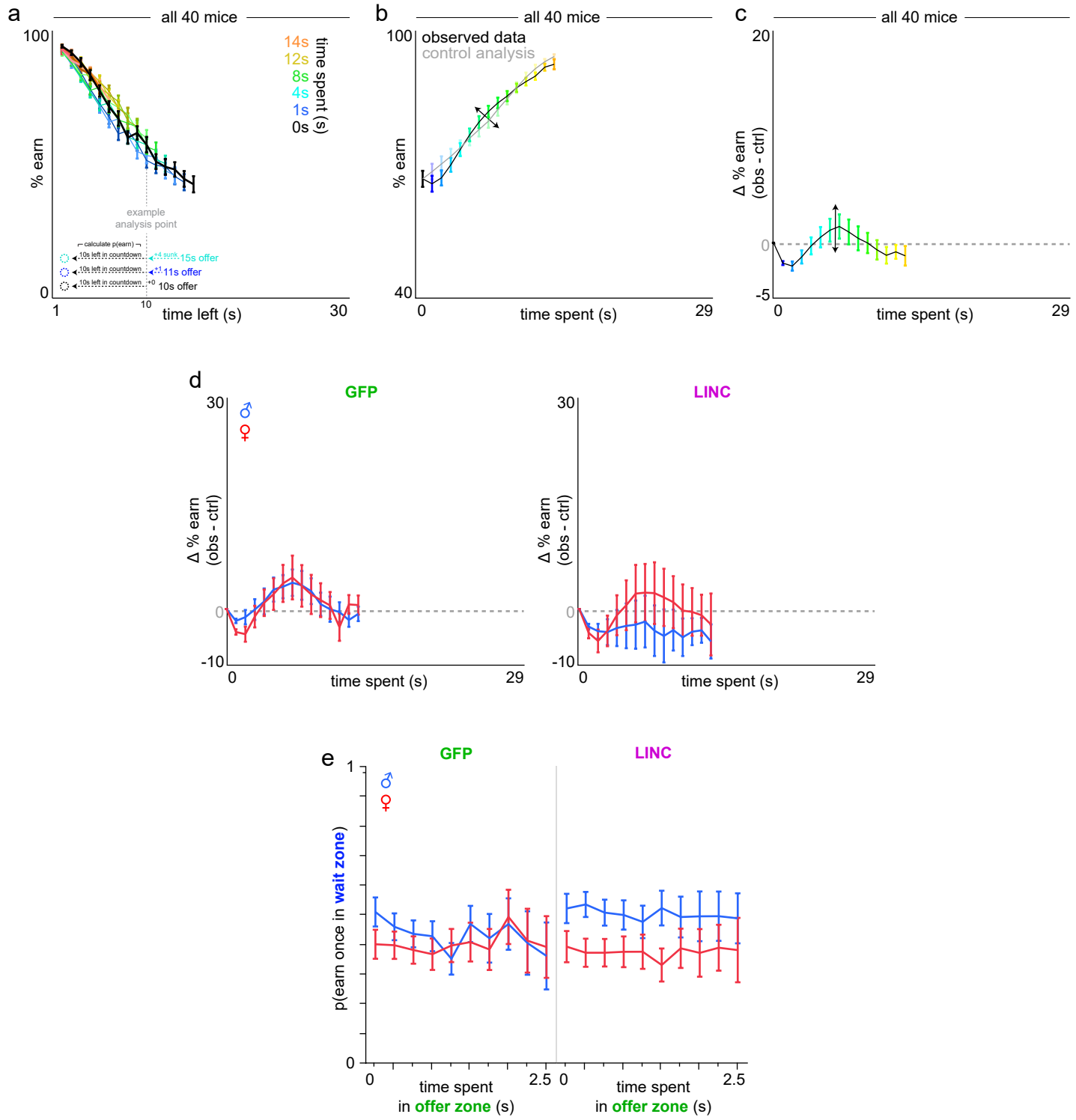

Supplementary Fig. 10 | Sensitivity to sunk costs analysis during the 1-15 s testing epoch. Mice do not display sensitivity to sunk costs during days 13-17 in a relatively reward rich environment compared to days 18+ (when offers range 1-30 s, as in main Fig. 5). **a-c** Sunk cost analysis of staying behavior in the wait zone, demonstrated using all 40 mice. (f) The likelihood of staying in the wait zone and earning a reward (e.g., not quit) is plotted as a function of time left in the countdown along the x-axis and time already spent waiting orthogonally in color. Note the black 0 s time spent curve represents animals having just entered the wait zone from the offer zone. Inset vertical dashed gray line illustrates an example analysis point comparing three sunk cost conditions originating from different starting offers but matched at 10 s left. Data from (a) dimensioned reduced in (b) collapsing across time left, highlighting the grand mean of each time spent sunk cost condition (color and x-axis). Difference between curves in (b) are plotted in (c) in order to summarize the envelope of the overall effect of time already spent on escalating the commitment of staying in the wait zone. Horizontal dashed line represents delta score of 0. **d** Data in (c) split by sex and virus treatment groups depicting no effect of time spent during the countdown in the wait zone on changing the probability of quitting vs. staying to earn a reward (time spent: F=0.522, p=0.470; sex*virus*time spent: F=0.809, p=0.369). **e** To compare to time spent waiting in the wait zone, data here depict a different type of time spent on the task: time spent in the offer zone prior to accepting an offer and entering the wait zone does not influence the probability of quitting vs. staying to earn a reward once in the wait zone (time spent in offer zone: F=1.574, p=0.210; sex*virus*time spent: F=0.916, p=0.339). These data are from the 1-30 s reward-scarce epoch (days 18-45) to demonstrate the unique value of time spent waiting in the wait zone uniquely conferring sunk cost sensitivity. Error bars represent ±1 SEM.

Supplementary Figure 11

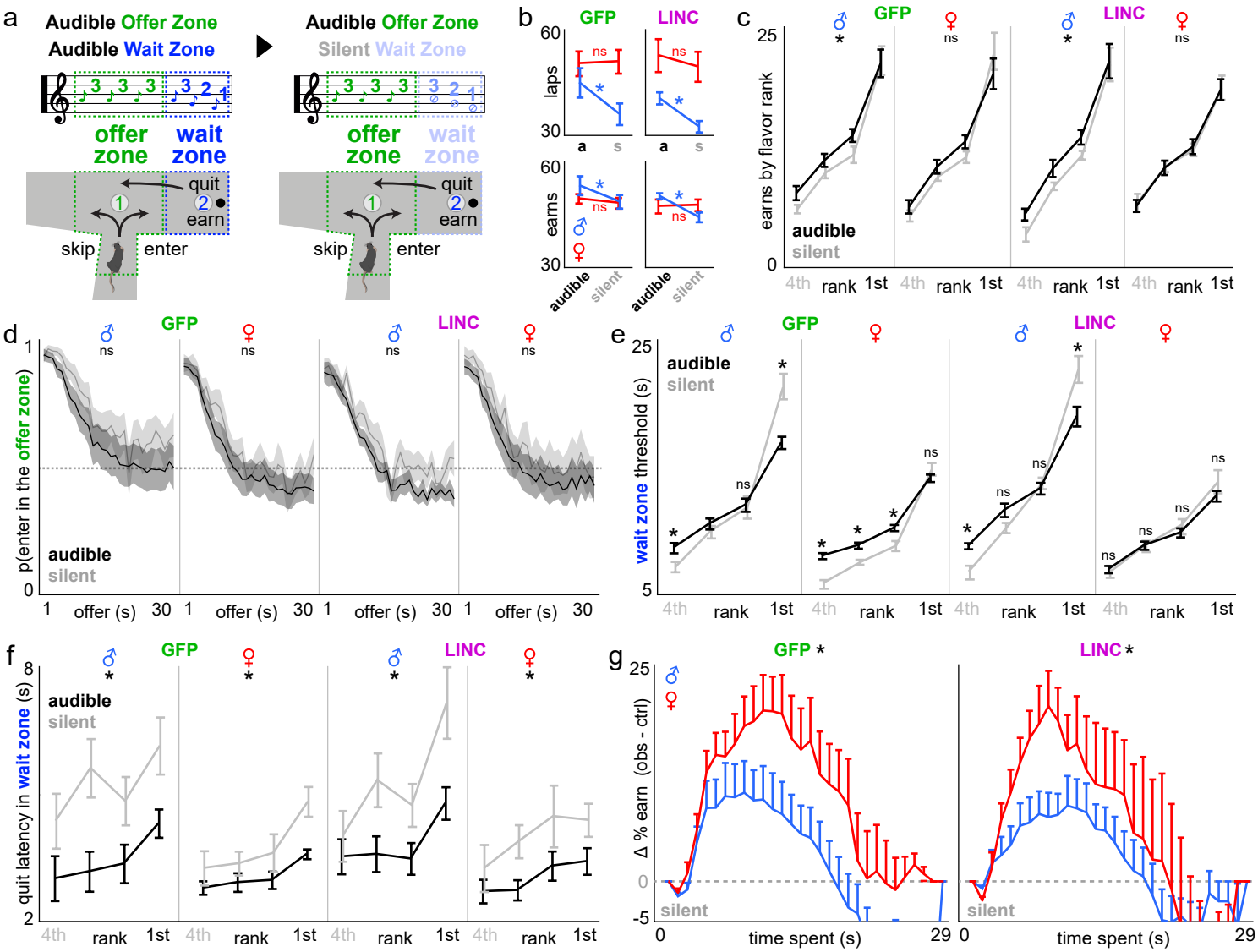

Supplementary Fig. 11 | Sex- and LINC00473-dependent wait zone behaviors are differentially modulated by access to specific task information. a Informational manipulation schematic: (left) standard Restaurant Row task followed by (right) two days of tones silenced only in the wait zone, but not offer zone (remains audible as before). **b** Total number of laps run in the correct direction (top) and total pellets earned aggregated among restaurants (bottom) across the audible and silent wait zone task conditions (x-axis). **c** Rewards earned in each restaurant ranked from least (4th) to most preferred (1st) across the audible (black) and silent wait zone (gray) task conditions. **d** Overall offer zone choice probabilities to make enter decisions as a function of audible cued offer costs collapsed across all flavors to illustrate no effect of task condition on auditory discriminatory behaviors. Horizontal dashed line indicates change at 0.5. **e** Wait zone thresholds in each restaurant across task conditions. **f** Latency to quit reaction times once in the wait zone in each restaurant across task conditions. **g** Sensitivity to sunk costs in the wait zone depicted here only in the silent condition as a function of time already spent (x-axis). Y-axis reflects delta earn probabilities as depicted in main Fig. 5h. Prominent sex-dependent effects of withholding wait zone information on overall task performance (observed in males), wait zone economic decision policies (bidirectional in males, unidirectional in GFP-females, and no effect in LINC00473-females), and sunk cost sensitivity (sex difference revealed for the first time GFP groups unlike in main Fig. 5). Horizontal dashed line indicates delta score of 0. ***** in (b-f) represent significant effects of task condition within group. * in (g) represent significant sex differences. Shading / error bars represent ±1 SEM. See **Supplementary Text**.

Supplementary Figure 12

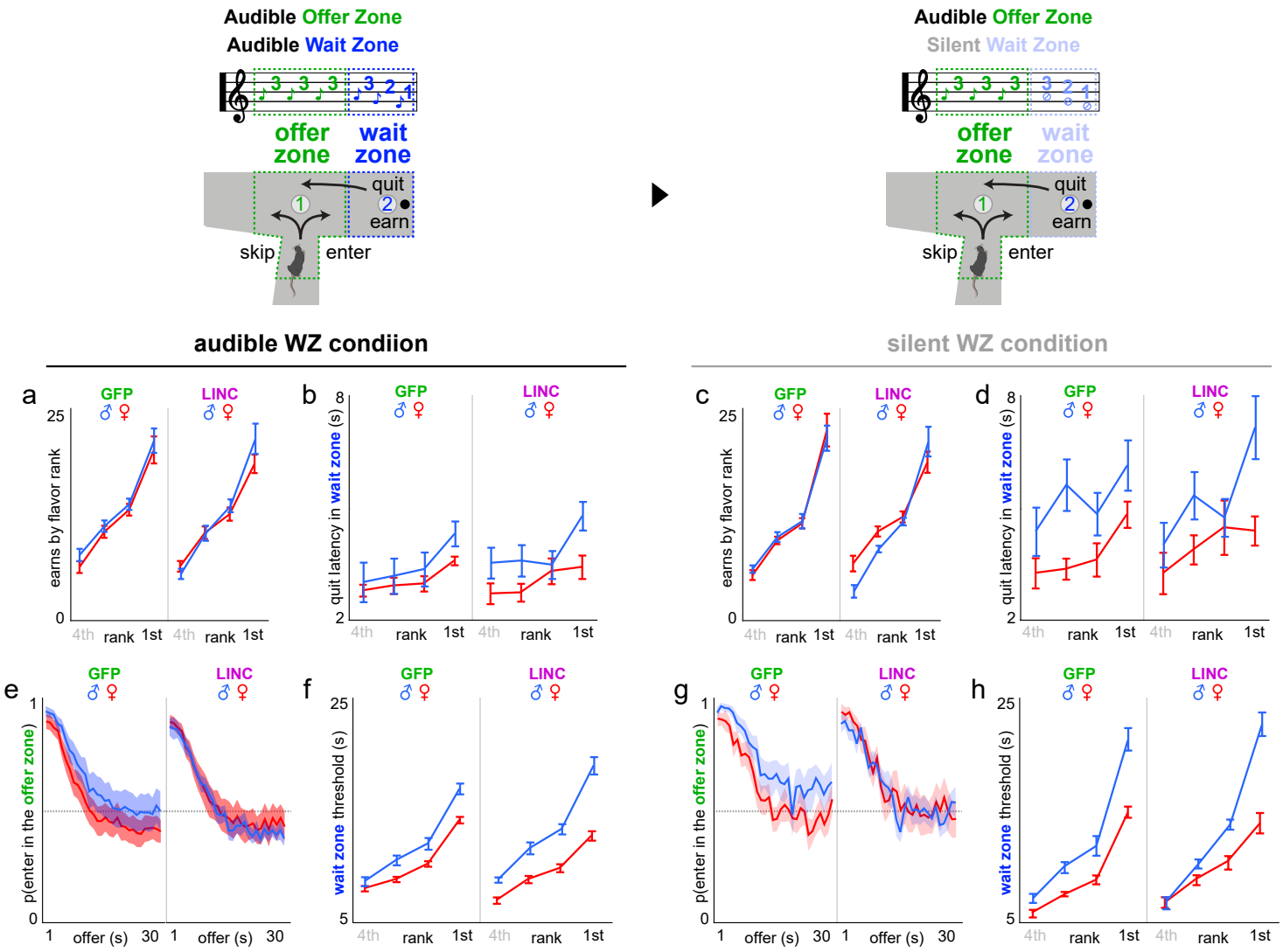

Supplementary Fig. 12 | Redisplay of main metrics obtained from task information manipulation. Figures redisplayed separating task manipulation conditions (baseline audible wait zone (WZ) vs. silent WZ conditions) and superimposing sex. Redisplay from Supplementary Fig. 11. **a,c** Average number of rewards earned split by flavors ranked from least to most preferred based on end-of-session totals. **b,d** Average latency to quit after accepting an offer once in the wait zone. **e,g** Average proportion of trials accepted by making an enter decision from the offer zone into the wait zone as a function of cued offer cost in the offer zone. **f,h** Average wait zone threshold calculated from the inflection point of Heaviside-step function fits to wait zone outcome (earn vs. quit) as a function of the starting delay of each trial. Error bars and shading represent ±1 SEM.

Supplementary Figure 13

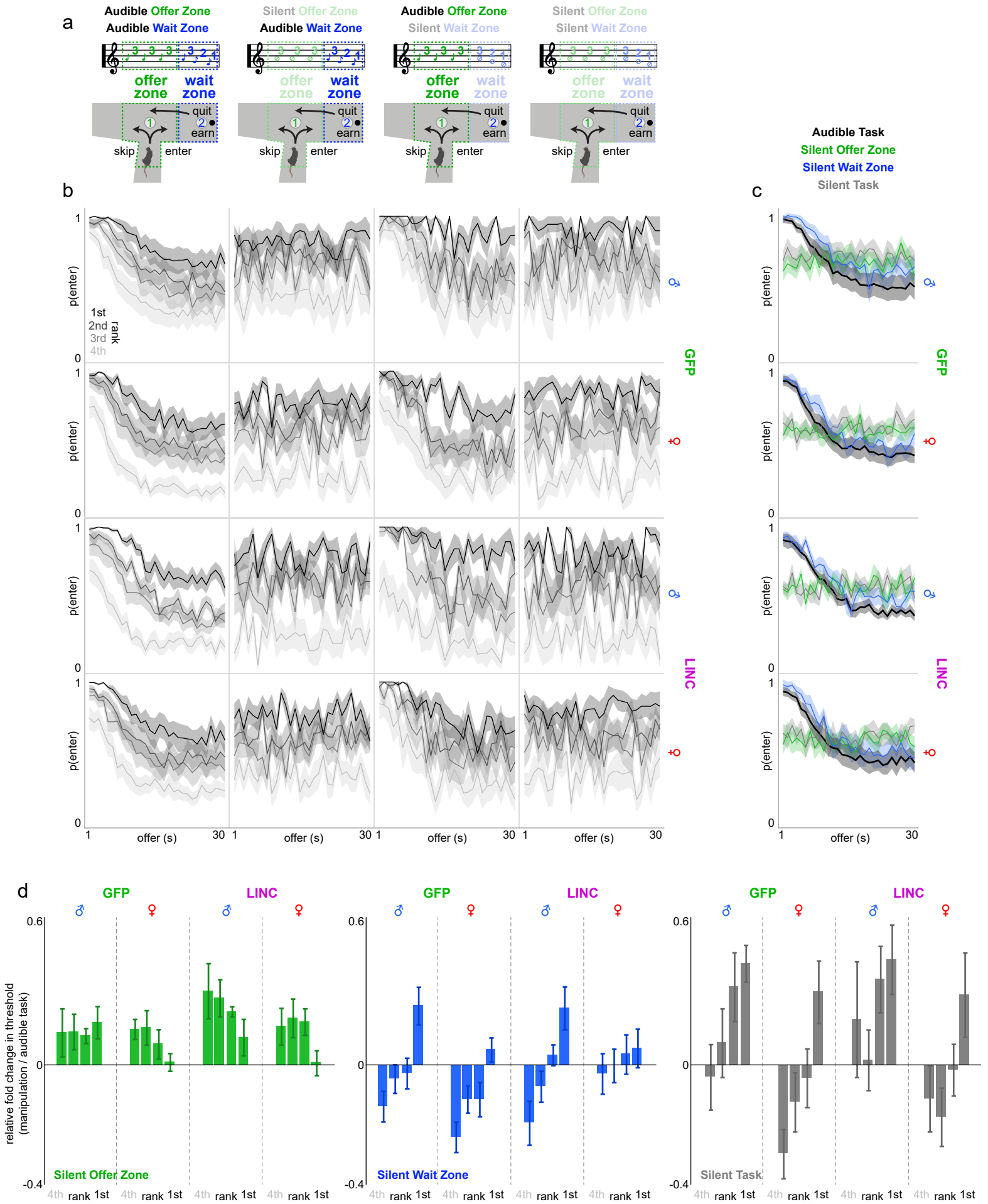

Supplementary Fig. 13 | Full set of task information manipulations on Restaurant Row. a After day 45, mice were challenged with special probe days on three different task informational manipulations each for 2 days. Manipulations took the form of silencing and withholding tone presentation either in the offer zone, wait zone, or both: (i) silent offer zone but audible wait zone [days 46-47], (ii) audible offer zone but silent wait zone [days 48-49], and (iii) silent offer zone and silent wait zone [days 50-51]. **b** Offer zone choice probability to enter as a function of offer cost split by restaurants ranked from least (4th) to most (1st) preferred separating sex and virus treatment groups (rows) across the 4 different task information conditions (columns). **c** Data in (b) collapsed across all four restaurants showing summary enter probabilities as a function of offer cost. Note that enter probabilities are largely unaffected when the offer zone tones are audible comparing baseline (black, regular task) to silent wait zone (blue) conditions, however, as intended, offer zone choice probabilities change into a flat horizontal line in both the silent offer zone (green) and silent task (gray) conditions, as animals do not have any tone information in the offer zone during these conditions (audible task: offer: F=2017.115, p<0.0001; sex*virus*offer: F=1.912, p=0.167; silent offer zone task: offer: F=1.783, p=0.182; sex*virus*offer: F=0.227, p=0.634; silent wait zone task: offer: F=1004.552, p<0.0001; sex*virus*offer: F=0.147, p=0.702; fully silent task: offer: F=0.723, p=0.395; sex*virus*offer: F=1.723, p=0.190). **d** Wait zone thresholds plotted as a relative fold change comparing each condition to the regular task audible baseline separated across the three information manipulations (silent offer zone, left, green; silent wait zone, middle, blue; silent task, right, gray) split by restaurants ranked from least (4th) to most (1st) preferred, sex, and virus treatment groups. Note the difference in patterns in changes in wait zone thresholds across restaurants between sex/virus groups and across task information manipulation conditions. Sign tests: silent offer zone: male GFP: least preferred: t=+1.365, p=0.103; most preferred: t=+2.639, p<0.05; male LNC: least preferred: t=+2.699, p<0.05; most preferred: t=+1.538, p=0.079; female GFP: least preferred: t=+3.638, p<0.01; most preferred: t=+0.360, p=0.363; female LNC: least preferred: t=+2.125, p=<0.05; most preferred: t=+0.188, p=0.427; silent wait zone: male GFP: least preferred: t=-2.684, p<0.05; most preferred: t=+3.191, p<0.01; male LNC: least preferred: t=-2.624, p<0.05; most preferred: t=+2.685, p<0.05; female GFP: least preferred: t=-4.733, p<0.001; most preferred: t=+1.325, p=0.109; female LNC: least preferred: t=-0.411, p=0.345; most preferred: t=+0.886, p=0.199; silent task: male GFP: least preferred: t=-0.358, p=0.364; most preferred: t=+5.554, p<0.001; male LNC: least preferred: t=+0.794, p=0.225; most preferred: t=+3.049, p<0.001; female GFP: least preferred: t=-3.584, p<0.01; most preferred: t=+2.345, p<0.05; female LNC: least preferred: t=-1.009, p=0.170**;** most preferred: t=+1.671, p=0.064. Shaded area and error bars represent ±1 SEM. See **Supplementary Text**.

Supplementary Figure 14

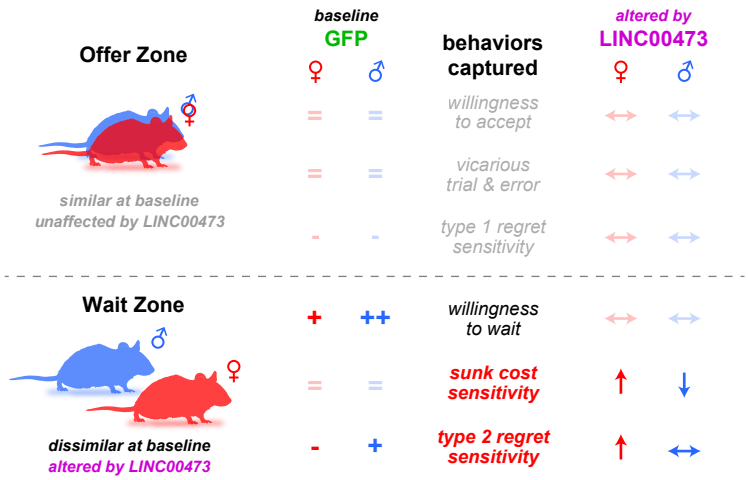

Supplementary Fig. 14 | Expansion of summary of key findings. Expanded table from main Fig. 6 describing in more detail the direction of baseline effects (GFP group) with equal signs (=) if no sex differences, plus signs (+ or ++) to represent a sex difference in magnitude, or minus signs (-) to indicate baseline insensitivity to a given behavioral metric. Metrics altered by mPFC LINC00473 expression are represented by arrow symbols showing either an increase (↑), decrease (↓), or no change (↔) relative to baseline. Bolded / opaque symbols highlight several key wait zone decision-making behaviors that are different between sexes at baseline or altered by LINC00473 expression, none of which appear in the offer zone.